CO_2 INJECTION IN UNCONVENTIONAL RESERVOIRS:

CHICONTEPEC TURBIDITES CASE STUDY

A Thesis

by

URIEL SALAZAR VERBITZKY

Submitted to the Office of Graduate and Professional Studies of
Texas A&M University
in partial fulfillment of the requirements for the degree of

MASTER OF SCIENCE

Chair of Committee,	David S. Schechter
Co-Chair of Committee,	Maria A. Barrufet
Committee Members,	Zenon Medina-Cetina
Head of Department,	Daniel Hill

August 2016

Major Subject: Petroleum Engineering

ABSTRACT

New fracturing techniques have helped to unlock the once unrecoverable oil from unconventional reservoirs. Unfortunately, even with newer technologies, there are still resources in place that the industry is leaving behind mainly because there is a lack of understanding on how to efficiently exploit them. For example, while hydraulic fracturing may create the conduits for oil to flow, it may not be a readily applicable technology in a complex and highly heterogeneous media like the Chicontepec field in Mexico, and a need arises for EOR techniques to be studied.

This research focuses in simulating, history matching and analyzing a CO_2 pilot test executed in the Chicontepec field. Fluid compositions, lab tests, and reservoir properties are provided based on a 40 x 40 x 40 grid. Also, pressure and production data are available for the wells.

First, a fluid model is created and tuned to match the lab tests. Then the reservoir model is completed and upscaled to improve CPU performance while avoiding loss of accuracy. The history match honors CO_2 injection rates while retaining both pressure and rate control. Based on the best match, new scenarios are run to study the effect of different injection rates and volumes. Finally, dimensionless injection vs recovery curves are created based on simulation forecasting.

While the pilot test did not achieve the expected results, valuable insight was gained that will drive future projects. First, hydrocarbon pore volume injected (HCPVI) was too small to create a production response on off-set wells. Nevertheless, the extension

of the hydraulic fracture on the injector well plays a key role in the early breakthrough observed in the one and only well in which CO_2 breakthrough was observed. The geomechanical aspects of the fracture are not studied in detail but are proven to affect the numerical simulation. Finally, a few observations regarding the ideal data acquisition program are provided.

DEDICATION

For a brave woman, who has traveled the world with me with no hesitation.

For a joyful lady, who makes me smile when times are difficult.

For a beautiful person, who finds her way to make our lives always enjoyable.

For my lovely wife.

Always.

ACKNOWLEDGEMENTS

I would like to thank my committee chair, Dr. David S. Schechter for his support and guidance throughout my master studies, I am sure that you will find a part of him in this thesis. Also, my committee co-chair, Dr. Maria A. Barrufet, whose vocation exceeds the standards. Similarly, Dr. Zenon Medina-Cetina, for his recommendations to my work. Thanks also to my professors at Texas A&M, specially Dr. Tom Blasingame and Priscilla G. McLeroy.

I also want to extend my gratitude to Petróleos Mexicanos (PEMEX), Secretaria de Energia (SENER) and Consejo Nacional de Ciencia y Tecnologia (CONACYT) for funding my studies and providing most of the data. I am proud to be part of one of the biggest National Oil Companies and for being honored with their support.

I would like to acknowledge Dr. Fernando Samaniego and Dr. Heber Cinco for writing my letters of recommendation. Also, a special mention to Dr. Edgar Rangel, a great person that we will always remember for his willing to help the others.

Thanks also to my good friends: the *Wettability*, the *Latinos* and Dr. Schechter's research group. Most of us will be able to work together again and some of us will not, but I will always cherish our experiences together.

Thanks also to my parents, who have always motivated me to go for the best.

Finally, thanks to my wife for her continuous support. Without her, this experience would not have been as enjoyable and fruitful as it has been. This is the result of both our efforts.

NOMENCLATURE

ATG	Aceite Terciario del Golfo
BHP	Bottom-hole Pressure
BT	Breakthrough
CCE	Constant Composition Expansion
CO_2	Carbon Dioxide
DL	Differential Liberation
EOR	Enhanced Oil Recovery
EOS	Equation of State
HCPV	Hydrocarbon Pore Volume
HCPVI	Hydrocarbon Pore Volume Injected
HM	History Match
IOR	Improved Oil Recovery
M (prefix)	Thousands
MM (prefix)	Millions
MMP	Minimum Miscibility Pressure
OOIP	Original Oil in Place
PEMEX	Petróleos Mexicanos
PVT	Pressure-Volume-Temperature
SA	Sensitivity Analysis
SI	International System (Units)

TABLE OF CONTENTS

Page

ABSTRACT ii

DEDICATION iv

ACKNOWLEDGEMENTS v

NOMENCLATURE vi

TABLE OF CONTENTS vii

LIST OF FIGURES ix

LIST OF TABLES xi

CHAPTER I INTRODUCTION 1

- Objectives 3
- Overview of Thesis Sections 3

CHAPTER II LITERATURE REVIEW 4

- Overview of Available EOR Methods 5
  - Thermal Methods 7
  - Non-Thermal Methods 10
- CO_2 Flooding 13
  - Minimum Miscibility Pressure 13
  - CO_2 Flooding Application 17

CHAPTER III NUMERICAL SIMULATION 22

- I/O Control 24
- Reservoir Properties 25
- Fluid Modelling 28
- Rock-Fluid Interaction 38
- Initial Conditions 41
- Numerical 42
- Wells, Completions and Production Data. 42
- Optimization 48

History Matching....50
Forecast and Post Simulation Analysis....59

CHAPTER IV CONCLUSIONS AND RECOMMENDATIONS....62

Conclusions....62
Recommendations....64

REFERENCES....66

LIST OF FIGURES

Page

Figure 1: Chicontepec reserves with respect to Mexican reserves as of January of 2015. (in MMboe).....2

Figure 2: Classification of EOR Methods. Adapted from Thomas .S (2008).....6

Figure 3: Diagram of the Slim Tube apparatus. Modified from Yellig and Metcalfe (1980).....14

Figure 4: MMP determination plot for a slim tube test.....15

Figure 5: Carbon dioxide flooding as a pilot test, modified from Mungan, N. (1982).....20

Figure 6: CO_2 pilot test timeline. 22

Figure 7: Original permeability cross section, in milidarcies (22^{nd} layer). Permeability heterogeneity and hydraulic fractures are visible. 23

Figure 8: Builder reservoir simulator settings.....24

Figure 9: Importing the RESCUE model, part 1 of 3.....26

Figure 10: Importing the RESCUE model, part 2 of 3.....26

Figure 11: Importing the RESCUE model, part 3 of 3.....27

Figure 12: Rock compressibility definition.....28

Figure 13: Unit and EOS definition. 30

Figure 14: Fluid composition. *Primary* refers to the reservoir fluid. *Secondary* to the injection fluid (CO_2) 31

Figure 15: Fluid regression block.....32

Figure 16: DL test data. A weighting factor of 5 in oil viscosity is set for viscosity matching purposes. 32

Figure 17: CCE test data. 33

Figure 18: Gas formation volume factor (Gas FVF).....34

Figure 19: Oil viscosity.....35

Figure 20: Relative volume from constant composition expansion (CCE) 35

Figure 21: Oil and gas specific gravities. Upper line corresponds to oil and the bottom line to gas. 36

Figure 22: Relative oil volume (ROV) and Gas-Oil Ratio (GOR). Upper line corresponds to ROV and bottom line to GOR. 36

Figure 23: Phase envelope, 10 pseudo-components 37

Figure 24: Phase envelope, 7 pseudo-components 38

Figure 25: k_{ro} and k_{rw} as a function of Sw 39

Figure 26: k_{ro} and k_{rg} as a function of Sg 40

Figure 27: Relative oil permeability as a function of fluid saturation. 41

Figure 28: Top view of the well arrangement in the numerical model. Each blue point represents a pair of (x,y) nodes, for each plane that the well crosses. 42

Figure 29: Well disposition and perforations in the final, optimized model. 43

Figure 30: Injection data for well 331ig (CO_2 injector) 47

Figure 31: Linear flow regression for well 332 52

Figure 32: Base case: calculated injection bottom hole pressure. Blue dots represent measured data, the yellow line the calculated BHP. 53

Figure 33: Hall plot for Well 331, CO_2 injector. 54

Figure 34: Hall plot theory, adapted from Jarrel and Stein (1991) 55

Figure 35: Well 331 injection BHP, CO_2 injector. Shaded in green the time frame at which the Hall plot suggests a change of injectivity. 56

Figure 36: History match, injection rate control. 57

Figure 37: History match, injection BHP control. 57

Figure 38: Cumulative CO_2 injected. HM scenario, pressure control. 58

Figure 39: Dimensionless recovery curve. 60

Figure 40: Production profiles for three injection rates. 61

LIST OF TABLES

Page

Table 1: Summary of results for calculated MMPs with different methods and correlations 16

Table 2: Summary of PVT properties 29

Table 3: Initial fluid composition 29

Table 4: Hydraulic fracture design summary. 44

Table 5: Monthly oil production 45

Table 6: Monthly gas production 45

Table 7: Monthly water production 46

Table 8: Monthly GOR 46

Table 9: List of modified numerical controls 49

Table 10: Summary of available data 50

Table 11: Oil recoveries from EOR, after 20 years of CO_2 Injection. 59

Table 12: Suggested data acquisition program 65

CHAPTER I

INTRODUCTION

In recent years, Chicontepec attracted the Mexican government attention due to its large reserves and the opportunity that it represents for reversing the declining production of the country. Nevertheless, and regardless of the large investments made by the national oil company (NOC) Petróleos Mexicanos (PEMEX), production in Chicontepec reached a shy production peak of 72,000 bpd in 2013 falling short from their production goals and followed by a steep decline in the following years.

Aceite Terciario del Golfo Project (ATG or Chicontepec) is located in the formerly Northern region of PEMEX, covering an area of 4,243 square kilometers. The Chicontepec project comprises 29 fields. As of December 31, 2014 (PEMEX, 2015), PEMEX had 4,506 wells completed with 2,414 of those producing. Also, proved reserves totaled 599.3 million barrels of crude oil and 946.8 billion cubic feet of natural gas, making total proven hydrocarbon reserves 797.9 million barrels of oil equivalent. Mexican proven reserves as of January 1st of 2015 were of 13,017 million barrels of crude oil equivalent (PEMEX, 2015), which implies that Chicontepec proven reserves accounted for 6% of that number (Fig 1). The importance of Chicontepec is more apparent in its 2P and 3P reserves, accounting for 50% of 22,984 MMboe and 45% of 37,405 MMboe of the Mexican share respectively. (PEMEX, 2015)

Figure 1: Chicontepec reserves with respect to Mexican reserves as of January of 2015. (in MMboe)

Steep decline rates, low initial pressures, tight oil characteristics and high uncertainty regarding the reservoirs hydraulic continuity are just a few of the technical problems that the field poses.

Objectives

Based on the information for the Chicontepec CO2 injection pilot test, executed between Jan 1st of 2010 and Jan 1st of 2011, the objectives of this study are:

- Perform compositional simulation of CO_2 flooding in turbidites as those of Chicontepec.
- Analyze the effects of CO_2 injection in thigh oil media.
- Analyze the effects of hydraulic fractures in the Chicontepec CO_2 flooding processes.
- Match and improve the fluid compositional model.
- Effectively reduce the layers of the simulation model without losing the heterogeneity of the model itself.
- Further understand the phenomena observed during the pilot test.
- Propose a general data acquisition program for future applications.

Overview of Thesis Sections

This thesis is divided into four chapters. The next chapter presents a literature review on CO_2 Enhanced Oil Recovery (EOR), with a brief overview of other available methods and definitions. Chapter 3 provides a detailed walkthrough of the numerical simulation, starting from the creation of the compositional model all the way up to history matching the CO_2 pilot test and forecasting new injection scenarios. The last chapter presents a series of conclusions and recommendations that should feed future EOR projects.

CHAPTER II

LITERATURE REVIEW

Enhanced Oil Recovery (EOR) processes are well known for their importance within petroleum engineering. It is important though, to define and differentiate a few concepts before understanding EOR. Usually, definitions change in some degree based on the source, i.e. financial or technical sources may slightly differ as well as those from service companies and the academia, nevertheless, we will find common ground within those definitions used by the experts.

Primary recovery is the first stage of oil and gas production, in which only natural reservoir drives (i.e. gas cap expansion) or some sort of artificial lifting system are involved into bringing the oil from the reservoir to the surface. Flowing wells or the use of artificial lifting systems are not exclusive to primary recovery processes, but are indeed the only operating wells at this stage.

Secondary recovery is usually, but not necessarily, the second stage of production in an oil and gas field. It is also known as pressure maintenance processes. Secondary recovery requires the injection of any non-reactive fluid into the reservoir, i.e. formation water or natural gas. The main goal is to increase or maintain the reservoir pressure as a means to add energy to it and keep the wells flowing for longer periods of time.

Tertiary recovery processes cover EOR methods, and they can be understood as a third production stage where miscible, chemical or thermal recovery processes are applied.

Then, the properties of the fluids and their interactions with the rock are modified, favoring oil and gas production.

Now, it is important to differentiate EOR from the concept of Improved Oil Recovery (IOR). EOR is a subset of recovery processes that may be thermal or non-thermal which aim to change the physical and chemical behavior of the reservoir fluids (Fig. 2). On the other hand, IOR refers to any process or technique to increase the oil recovery by any means. (Stosur *et al.* 2003) While the latter definition may include EOR processes, it is not restricted to it. For instance, Petroleum Reservoir Management (PRM) practices, horizontal wells or hydraulic fracturing are considered IOR.

Overview of Available EOR Methods

As seen in Fig. 2, there are several different EOR techniques which aim to change different fluid properties. In general, EOR methods may be classified as thermal and non-thermal.

Thermal methods are best suited for heavy, high viscosity oils. These methods supply heat to the reservoir, which vaporizes some fractions of the oil and reduces the viscosity, improving the mobility ratio. Other mechanisms, specific to the applied method, may be compaction, steam distillation, rock and fluid expansion and visbreaking.

Non thermal methods are usually applied in light oils with low viscosities, but may be applied to moderate viscosity oils where thermal processes may be unusable. As thermal methods, these aim to improve the mobility ratio, but also to lower the interfacial tension. The next few pages will give a more in depth description of both methods.

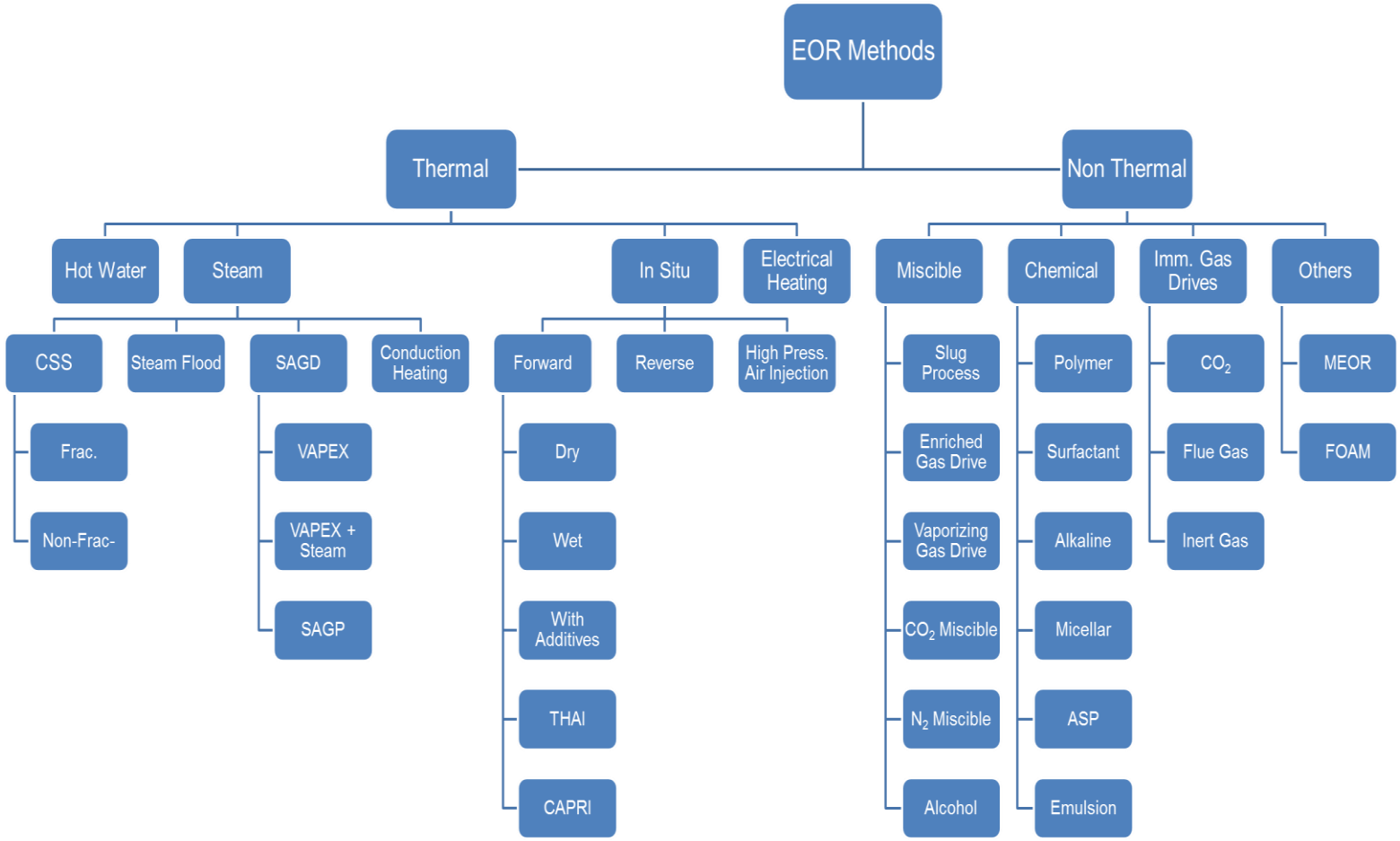

Figure 2: Classification of EOR Methods. Adapted from Thomas .S (2008)

Thermal Methods

Thermal methods have been studied and applied since the 50's (Thomas, S. 2008). Since the viscosity of the oil reduces as the temperature increases, these are more suitable for heavy oils (10-20 ºAPI) and tar sands (<10 ºAPI). These methods consist of supplying heat to the reservoir favoring the flow of oil. The source may be hot water, steam, electrical heaters or by creating an in-situ source.

To further understand their effects, it is important to understand the mobility ratio equation.

The mobility of a fluid (Eq. 1) is defined as the ratio of its relative permeability to its viscosity.

$$M_i = \frac{(k k_{ri})}{\mu_i} \qquad \text{(Eq.1)}$$

Then, a fluid mobility relates to the resistance to the flow resistance in a given rock (permeability and viscosity) at a given saturation of the fluid (relative permeability). One can observe from Eq. 1 that, since viscosity is in the denominator, low viscosity fluids (i.e. gases) have very high mobilities. M_i is inversely proportional to the fluid viscosity.

In displacing processes, the mobility ratio (Eq. 2) is defined as the mobility of the displacing phase divided by the mobility of the displaced phase. For example, in water flooding, the mobility ratio is calculated by dividing the water mobility to that of oil.

$$M = \frac{\frac{k_D}{\mu_D}}{\frac{k_d}{\mu_d}} = \frac{k_D \mu_d}{k_d \mu_D} \qquad \text{(Eq.2)}$$

In Eq. 2, *D* is the displacing phase, and *d* is the displaced phase.

It is important to observe that the mobility ratio equation is a relationship of the ability to move of the displacing phase to that of the displaced phase. Then, a high mobility ratio would imply sharp contrasts of mobility and, in the end, an unfavorable displacing situation.

Thermal methods will directly affect the oil viscosity (μ_d), lowering the mobility ratio and improving the overall efficiency of the displacing process.

Cyclic Steam Stimulation (CSS)

This is a single well process and consists of three stages: Steam Injection, Soaking and Production. First, steam is continuously injected for about a month. Secondly, the well is shut in to allow for a heat redistribution. In the third stage, the well is put on production until it declines up to a point where another Injection-Soaking-Production cycle is needed. The final number of cycles will depend on the well economics.

A variation of the CSS requires injection above the fracture pressure, creating fractures and potential communication among wells.

Steam Flooding

This process is similar to water flooding, where there is injection based on patterns. Steam is injected continuously, theoretically creating a steam zone which displaces the oil. Heavy oil is mobilized due to viscosity reduction.

Steam Assisted Gravity Drainage (SAGD)

SAGD is a process which relies in the gravity segregation of steam. It consists of a pair of parallel, horizontal wells situated in the same vertical plane and situated a few meters apart. The top well injects steam whereas the bottom one produces oil and water. Due to its lower density, steam rises to the top of the formation, creating a steam chamber. Low viscosity oil, as bitumen, will mobilize thanks to the heat and drain to the bottom producer well. Continuous steam injection will eventually create a bigger steam chamber and spread laterally, improving the overall recovery. A key property to the success of this method is high vertical permeability. Also, very low mobility oils benefit the most from this method, as higher mobility oils allow for the creation of steam channels rather than a steam chamber.

Needless to say, SAGD is a very energy intensive process.

In Situ Combustion

In this method, air is injected to burn about 10% of the in place oil to generate heat. Very high temperatures are generated, in the range of 450-600 ºC, then a very high viscosity reduction occurs near the combustion zone. Additives may be used with air to enhance heat recovery. Common problems are severe corrosion, toxic gas production and gravity override.

This process is thermally efficient as there are no major thermal losses within the reservoir or the wellbore.

Non-Thermal Methods

Non-Thermal methods are traditionally used in light oils, but may be applied in moderately viscous oils (<2000 cp), where thermal methods are not suitable (Thomas, S. 2008). These methods aim to lower the interfacial tension, and improve the mobility ratio.

Within these methods, there are three main categories which aim to improve different properties of the fluids, these are: miscible, chemical and immiscible gas injection.

Miscible Flooding

Miscibility develops whenever two miscible fluids come into contact. During a fluid flooding, the displacing fluid is miscible with oil at either first contact (single contact miscibility, SCM) or after multiple contact (multiple contacts miscibility, MCM).

Single contact miscibility implies that the displacing fluid and the oil are immediately miscible. On the other hand, multiple contact miscibility requires a little more time to develop, as there is a continuous vaporization/condensation process between the two fluids until miscibility is achieved.

The theory suggests that there is a narrow transition zone, also known as mixing zone, where there is a steep change in the concentration of the displacing fluid.

Miscible flooding has gained a lot of traction, allowing for the development of different techniques, such as:

- Miscible slug process
- Enriched gas drive

- Vaporizing gas drive
- High pressure gas injection (CO_2, N_2)

Miscible flooding reduces interfacial tension. Also, if the mobility ratio is favorable (M<1), then the displacement efficiency approaches 1. This would mean that in a controlled environment, where the mobility of the displacing fluid is equal or less than that of the oil, there would be a perfect displacement of the oil and the maximum recovery would be achieved.

Chemical Flooding

Chemical flooding, as it name suggests, uses a mixture of chemicals as displacing fluid, creating a more favorable mobility ratio and/or increasing the capillary number (N_C).

It is important to understand their effect on the capillary number. (Eq. 3)

$$N_C = \frac{\mu U}{\sigma} \qquad \text{(Eq.3)}$$

Where:

N_C is the capillary number

μ is the fluid´s viscosity

U is the fluid´s velocity

σ is the fluid´s interfacial tension

As seen in Eq. 3, as the interfacial tension decreases, the capillary number increases. This would improve the displacement efficiency. For instance, if the interfacial

tension is zero, that would mean that the fluids are miscible and then, at least in theory, the displacement would be ideal.

Chemical processes include polymer flooding, surfactant flooding, micellar flooding, Alkali-surfactant-polymer flooding (ASP) and a combination of them.

Other Forms of Chemical Flooding

These include combinations of the traditional chemical processes with some other form of EOR, such as Surfactant-Steam flooding or a Steam-Foam combination, and more specific methods, like microbial or foam flooding.

In general, the microbial method consists of injecting indigenous or exogenous microbes which react with a carbon source, producing several organic and inorganic compounds. The recovery mechanisms are very similar to that of chemical EOR, such as interfacial tension reduction, improved mobility ratio, viscosity reduction, oil swelling and a notable increase in reservoir pressure, due to the formation of gases.

Foam flooding consists of the simultaneous injection of gas and surfactant into the porous media, to create an in-situ foam which form, breaks and re-forms. Since the mobility of foam is lower than that of the usual displacing gases, it acts as a viscous fluid. One of the major problems with foam is its stability and as of now, several institutions direct their efforts to address this issue.

CO_2 Flooding

CO_2 is a colorless, odorless, incombustible gas formed during respiration, combustion and organic decomposition (American Heritage Dictionary of the English Language, 2011) with the added benefit of being an efficient oil displacing agent. Depending on the oil composition and the injection´s pressure and temperature, the CO_2 might be single contact miscible, multiple contact miscible or not being miscible at all.

CO_2 flooding overall efficiency benefits from the following effects:

1. Oil viscosity reduction: In general, the more viscous the oil, the greater the reduction of viscosity.
2. Oil swelling: Oil swells as CO_2 is dissolved into it, increasing its volume based on temperature, pressure, oil composition and dissolved CO_2 mole fraction.
3. Miscibility effects (view minimum miscibility pressure next)
4. Increase of injectivity.
5. Dissolved CO_2 creates a solution gas drive displacement mechanism.

Minimum Miscibility Pressure

CO_2 Minimum Miscibility Pressure, or MMP, is defined as "the lowest pressure at which the CO_2-containing injection fluid can develop miscibility with the reservoir crude oil at reservoir temperature" (Mungan, N. 1981)

If the MMP is achieved, a favorable set of relative permeabilities develop allowing for additional recovery than the one obtained from only swelling effects.

Now, to determine the MMP, conventional PVT cells or slim-tube measurements may be used, with the latter holding significant advantages over the PVT cell. Fig.3 is a schematic of the MMP apparatus.

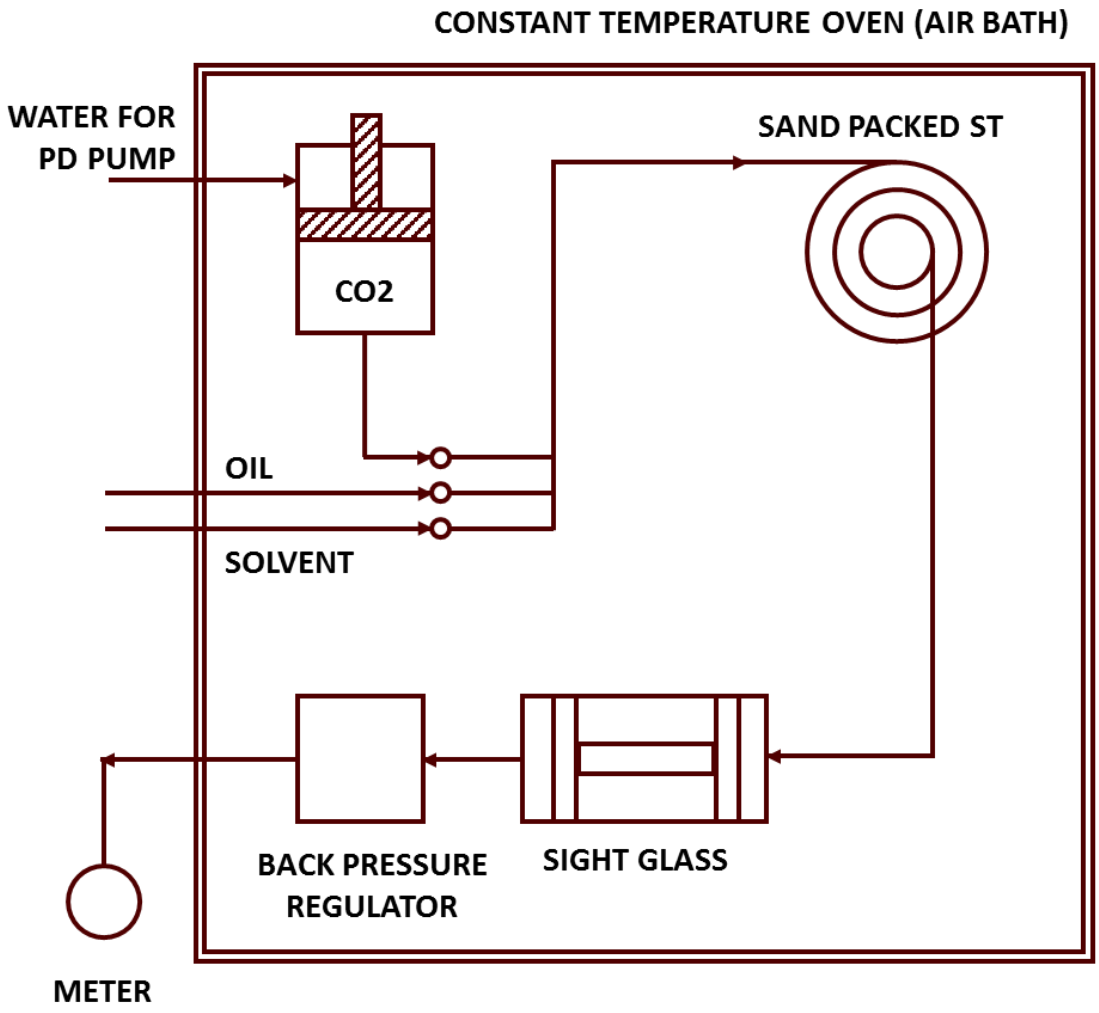

Figure 3: Diagram of the Slim Tube apparatus. Modified from Yellig and Metcalfe (1980)

The basic procedure consists of fairly straightforward steps. First, the slim tube is cleaned and dried with the use of solvent (i.e. Toluene) and CO_2. Then the system is

saturated with oil, heated and pressurized to the desired conditions. Next, CO_2 is injected at a low rate of around 0.06 cc/min to displace oil out from the sand packed slim tube, while recording the injected volumes against the recovered oil. Finally, at 1.2 pore volumes injected (PVI) or near 100% recovery, injection is stopped. The test is run several times at different injection pressures to allow for a clear inflection point to show, as observed in Fig. 4. The point where the two straight lines that pass through the data points meet is the MMP.

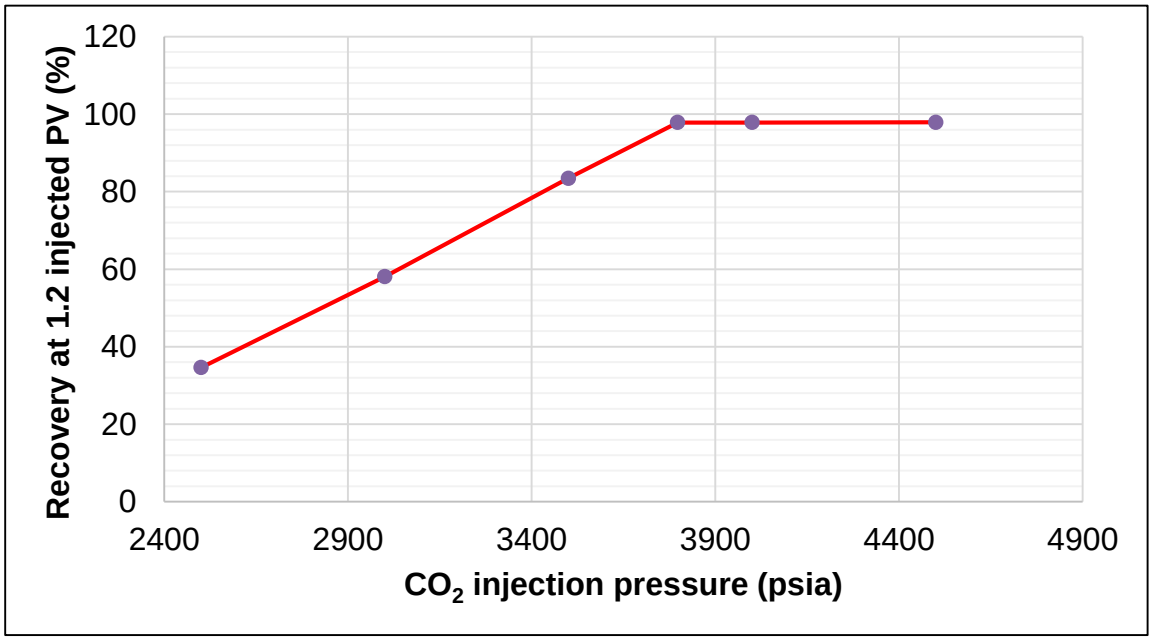

Figure 4: MMP determination plot for a slim tube test.

For quick screening calculations, correlations may be used but we do not advise to heavily rely on them, as the numbers may not be reliable at all. If lab tests are not available, MMP simulation usually obtain more consistent results than those of correlations. Table

1 is a summary of MMP calculations for different degrees of pure and impure streams, CO_2 included, comparing correlations and MMP simulations in a commercial simulator.

Table 1: Summary of results for calculated MMPs with different methods and correlations

METHOD / CORRELATION	PURE CO_2		CO_2/N_2 (15%)		CO_2/N_2 (85%)		C_1	
Yellig and Metcalfe	3,052.1	psia	32,908.7	psia	5,347.6	psia	21,374.7	psia
Glaso	2,562.0	psia	27,624.6	psia	4,488.9	psia	17,942.5	psia
Cronquist correlation	2,940.6	psia	31,707.3	psia	5,152.4	psia	20,594.3	psia
Dindoruk, etal	2,487.0	psia	2,915.2	psia	2,562.5	psia	2,990.8	psia
PVTsim	2,352.2	psia	6,298.4	psia	2,982.8	psia	4,216.8	psia

It is worth noting how different the results are, being PVTsim the reference result. This is due to the nature of the conditions at which these correlations where created. For instance, Yellig and Metcalfe (1980) developed a correlation to calculate the MMP for a pure CO_2 stream based solely on the temperature, yielding abnormal results for other compositions or mixtures. Similarly, Glaso also bases the calculations on the temperature but he also considered the influence of the C_2-C_6 mol fraction of the oil. We observe that, while Dindoruk provides consistent results, it does not work very well for any other stream than pure CO_2.

CO_2 Flooding Application

Studying, planning, executing, monitoring and diagnosing a field size CO_2 flooding requires the interaction of several disciplines, reservoir engineering included. Mungan, N. (1982) paper provides a comprehensive guide to the application of CO_2 in a field. We will use that paper as a guide for this section.

Selecting a Suitable Reservoir

In general, screening criteria is available for applying any available technology or process, such as when selecting the ideal artificial lift for your wells or a suitable EOR process. Nevertheless, if only a few available reservoirs are under our management, the first aspect to consider is whether the CO_2 displacement will be miscible or immiscible under reservoir conditions. The miscibility pressure will determine the required injection pressure and other aspects, as the age of the field, may oppose it. For instance, in old wells the injection may cause casing or cement failure.

Secondly, we must answer the following question: Will the flooding be horizontal or vertical? Vertical floods will benefit from gravity segregation, while horizontal floods will need strict mobility control to improve the potential results.

A third aspect considers reservoir heterogeneities. For instance, some horizontal floods could benefit from lateral permeability barriers.

Additionally, a series of specific considerations should be acknowledged, for instance:

1. Structural, geological and petrophysical characteristics could favor or negatively affect the flooding.
2. Gravity stabilized, miscible CO_2 floods perform better on thick pay zones.
3. Low permeability reservoirs with asphaltic crude oils do not perform well under a CO_2 flooding.
4. Availability of CO_2 plays an important role in the economics.

Determination of CO_2 Requirements

It is important to determine the volume of the CO_2 bank to be injected, assuming that the injection scheme is not continuous, but rather a CO_2 followed by water injection scheme. The CO_2 bank should be sufficiently big to maintain a CO_2 fluid between the oil bank (displace fluid) and the displacing fluid, such as water.

Oil Recovery Efficiency

The oil recovery calculations will come from two parts:

1. Recovery from the miscibly displaced zone.
2. Recovery from the "not prevailing miscibility" zone.

The recovery for the zone where the miscibility is not fully achieved is calculated as with any other method, like water flooding or gas injection. It is worth noting that the effects of oil swelling and viscosity reduction should be taken into account.

The calculation of the miscibly displaced zone depends on three calculations:

1. Displacement efficiency.

2. Areal sweep efficiency.
3. Swelling effect.

The first is fairly straightforward, as the efficiency for miscible floods in CO_2 is considered to be over 95%, due to its nature as a miscible flood and the effects of swelling and viscosity reduction.

The areal sweep may be calculated from prior works, such as those of Claude and Witte (1959). It considers the relationship between the areal efficiency and the viscosity ratio at breakthrough

Similarly as any other EOR process, the vertical conformance can be accurately estimated from the work of Lorenz and his coefficient of heterogeneity.

Then, the overall efficiency is a result of Eq. 4 and Eq. 5:

$$E_t = E_i V_i + E_m V_m + E_s \quad \text{(Eq.4)}$$

$$E_m = e_d e_a e_v \quad \text{(Eq.5)}$$

Where:

E_t : Overall oil recovery efficiency, % HCPV

E_i : Oil recovery efficiency for immiscible displacement

V_i : Hydrocarbon pore volume in immiscibly displaced zone [fraction]

E_m : Oil recovery efficiency for miscible CO_2 displacement

V_m : Hydrocarbon pore volume in miscibly displaced zone [fraction]

E_s : Oil recovery due to swelling, % HCPV

e_d, e_a, e_v : displacement, areal and vertical sweep efficiencies, respectively [fraction]

Pilot Testing

It is a widely accepted practice that before embarking into a field scale flooding, one should perform a pilot test to prove the applicability of the process and to learn about any potential operational and field problems that may have not been anticipated in the lab.

Figure 5: Carbon dioxide flooding as a pilot test, modified from Mungan, N. (1982)

Fig. 5 shows a general schematic of a CO_2 flooding pilot test. The preflush is usually used to raise the reservoir pressure to the MMP. Tracers should be injected along with the CO_2 to provide a reliable tracing agent since they will provide valuable information on the movement of the fluids and the sweep efficiency. The chase fluid could be water or any inexpensive gas that it is available.

Problems in the Field

The usual problems encountered during CO_2 flooding are:

1. Corrosion
2. Asphaltene deposition
3. CO_2 handling

Corrosion is a serious problem in the field. Since CO_2 and water form carbonic acid, it creates a very corrosive environment for steel. This problem is more evident in alternating water/gas schemes. Fortunately, the use of stainless steel wellhead and equipment, along with separate injection facilities for water and CO_2, will significantly reduce the effects of corrosion.

Asphaltene deposition will occur on highly asphaltic crudes and low permeability formations. Laboratory tests should be able to show if this problem will be serious or not.

CO_2 handling can be compensated if most of the CO_2 is reinjected, thus reducing the amount of CO_2 that needs to be purchased.

CHAPTER III

NUMERICAL SIMULATION

A pilot CO_2 flooding test was conducted in a Chicontepec field. The CO_2 was injected following an inverted seven spot injection pattern with 400 m (1312 ft) spacing between wells. All but one offset well are hydraulically fractured, with fracture planes oriented N (27° ± 3) E.

The general timeline of the pilot test is shown in Fig. 6.

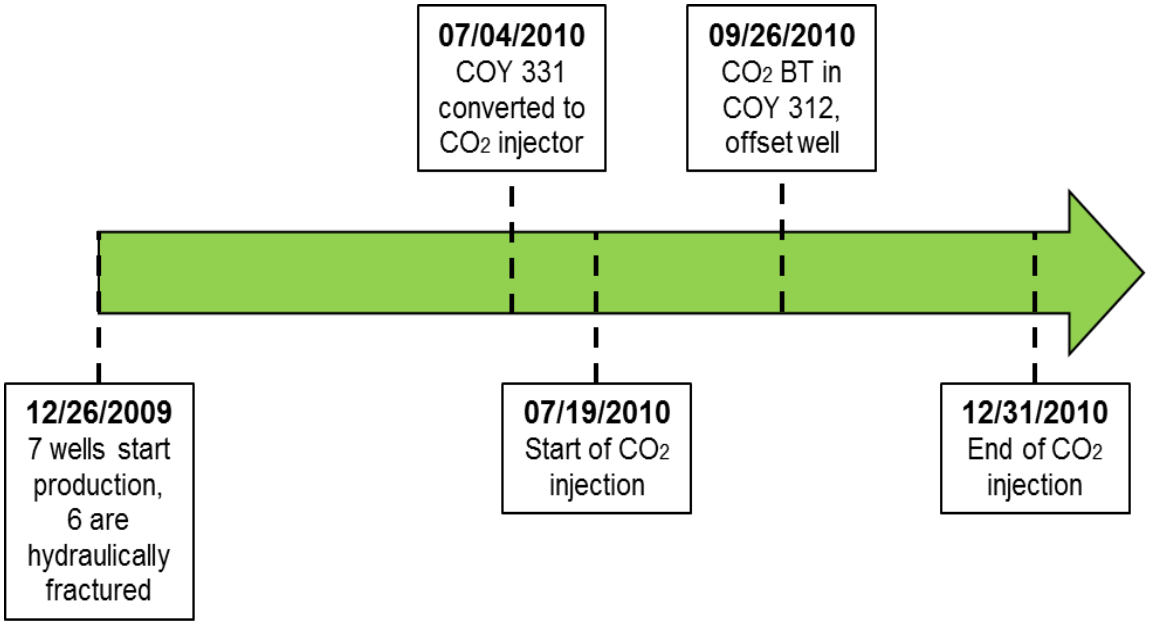

Figure 6: CO_2 pilot test timeline.

The seven wells were drilled and put into production in December of 2009. Curiously, 6 out of 7 wells were hydraulically fractured, excluding an offset well but not the future CO_2 injector. Given the orientation of the fracture planes, the simulation

explores the scenario of an alignment between the fracture planes of the injector well and two offset wells (Fig. 7). It is believed that this promoted early breakthrough (BT).

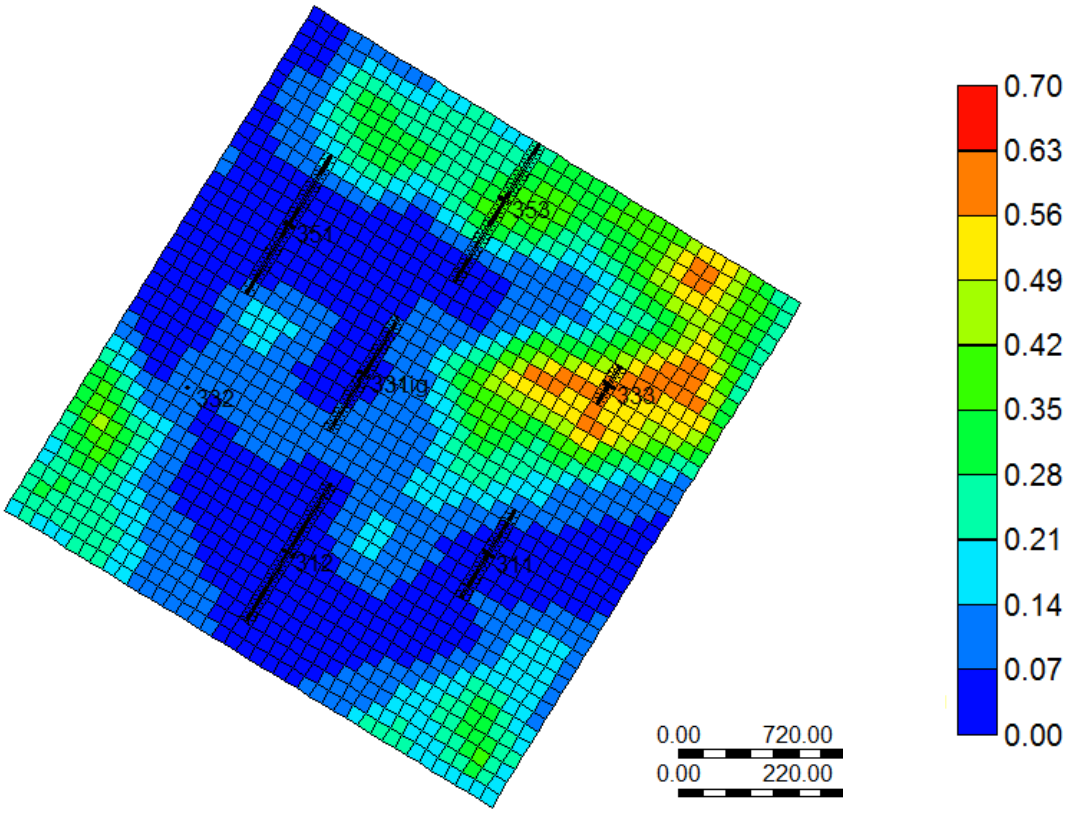

Figure 7: Original permeability cross section, in milidarcies (22nd layer). Permeability heterogeneity and hydraulic fractures are visible.

Reservoir simulation is used to further understand the reservoir phenomena and how it affected field observations. History match is performed honoring the bottom-hole pressure (BHP) of the injection well and forecast is run over the best match.

Most of the work was done in the CMG simulation suite (2013), specifically GEM (Compositional simulation), WINPROP (Fluid modelling), CMOST (Computer assisted

history matching, optimization & uncertainty analysis) and the Results application, nevertheless, additional references to Petrel and Eclipse, by Schlumberger, will be found. This chapter is a step by step description of the compositional simulation workflow and we hope it serves as a guide for future work.

I/O Control

When initiating the CMG simulation suite, the easiest way to start building a simulation model is by using Builder. Immediately after clicking on it, it will ask for a few simulation essentials: Are we performing a black oil, compositional or thermal simulation? Will the input data will be on SI or Field units? Is it a single porosity or dual porosity model? Fig. 8 shows the specifics for this simulation model.

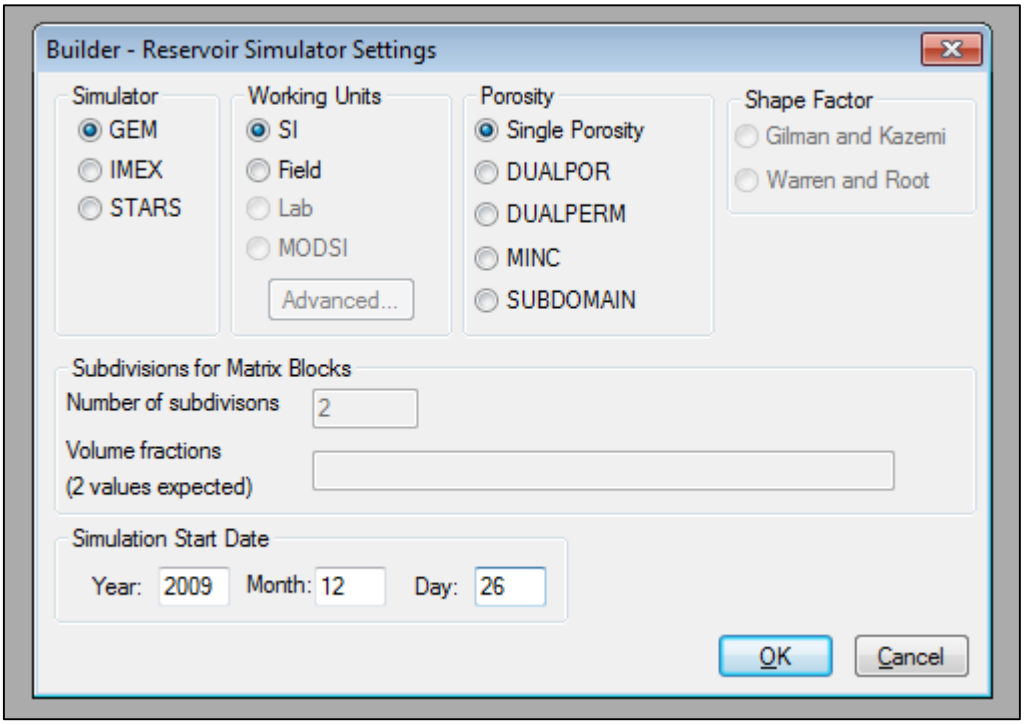

Figure 8: Builder reservoir simulator settings.

No additional actions are needed at this stage in order to clear the requirements for moving to the next step. However, additional options like *Restart*, which creates a restart file for forecasting, are under the *I/O Control* tab.

Reservoir Properties

Simulation properties like the number of grid blocks and their geometry are defined here. Also, the following reservoir properties are defined: porosity (ϕ), permeability (k), net to gross ratio, null blocks and rock compressibility (c_r).

Most of these properties are imported from a RESCUE file, generated in PETREL. It is important to acknowledge that the grid comes from PEMEX's Chicontepec project and properties like the permeability/porosity distributions are generated based on well logs and a geostatistical model, therefore we do not have a perfect, symmetrical grid. In general, geostatistical modelling bases itself in well logs and cores, when available. A "seed" is planted, with known properties at known locations, and using stochastic modelling techniques, property distributions are created for the rest of the reservoir.

Importing the RESCUE model is fairly straightforward (Fig. 9, 10 and 11). However, it is important to understand the equivalence between Schlumberger's Eclipse and CMG's GEM keywords. Porosity and permeability are easily translated, but others like the net to gross ratio (GEM: NETGROSS > Eclipse: VSHALE) are not so obvious and may require some preconditioning. Furthermore, NULL Blocks (GEM) may not be directly translated, but rather activated/deactivated with the use of the ACTNUM keyword (Eclipse). This step is shown in Fig. 11.

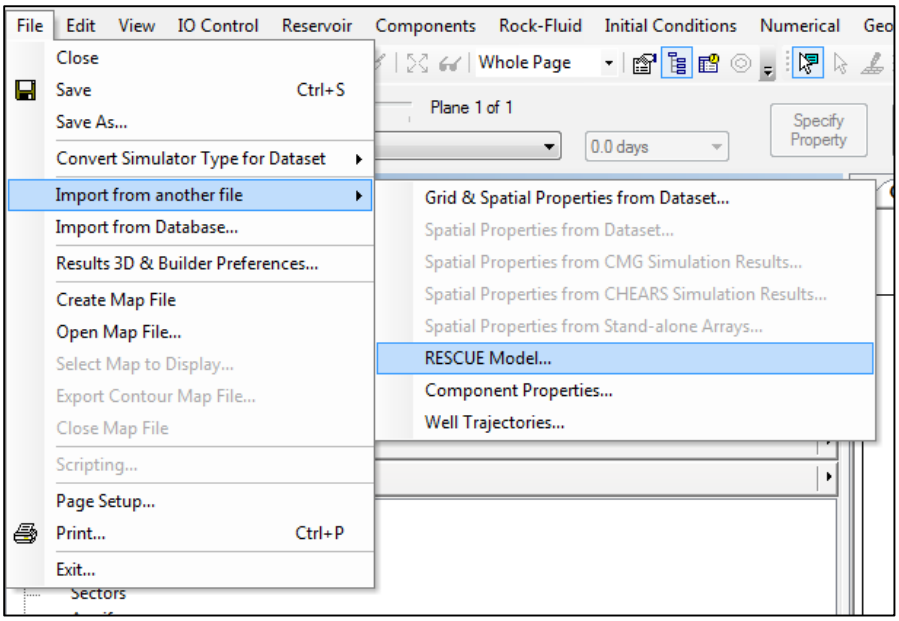

Figure 9: Importing the RESCUE model, part 1 of 3.

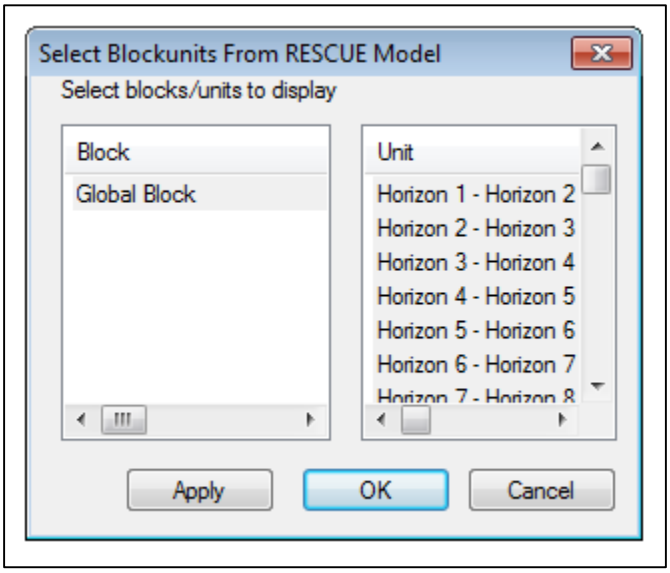

Figure 10: Importing the RESCUE model, part 2 of 3.

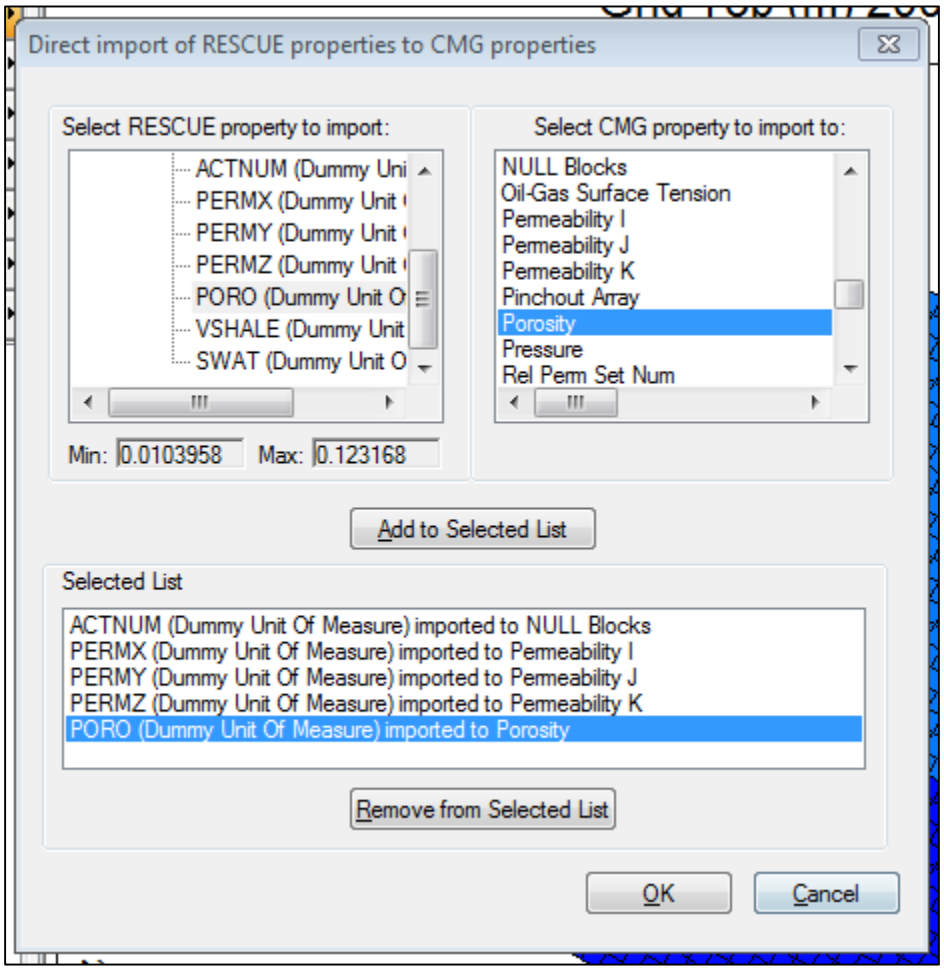

Figure 11: Importing the RESCUE model, part 3 of 3.

The rock compressibility (c_r) is part of the known properties of the reservoir (Fig. 12). Since this simulation model is in SI units, there is a need to translate the compressibility from the 0.1312 x10-6 psi to 0.019x10-6 kPa. This will be a continuous issue throughout the building process because we imported the RESCUE file, which includes the grid properties in SI units (i.e. meters), and it is unavoidable.

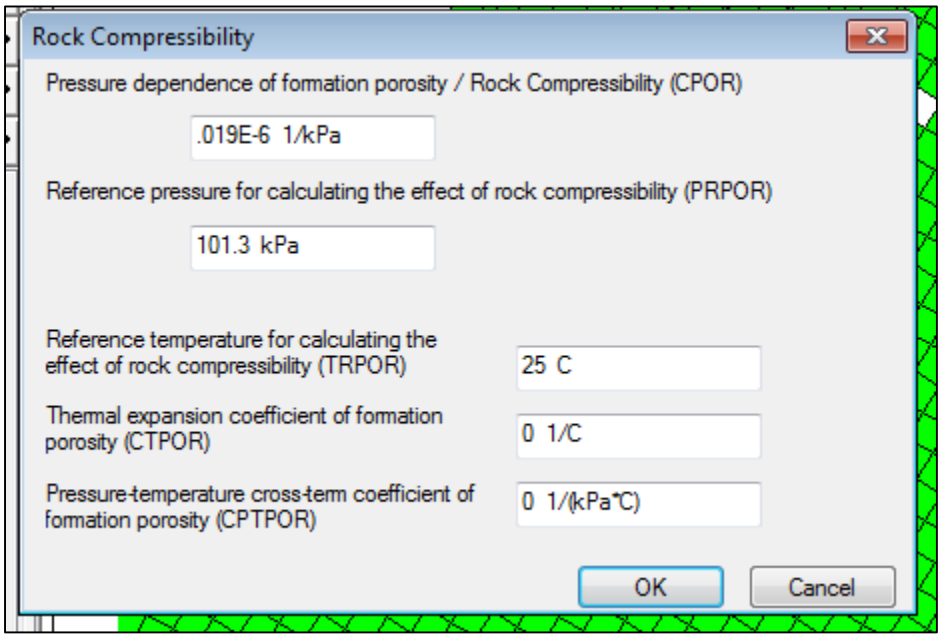

Figure 12: Rock compressibility definition.

This should lift any restrictions or warnings from the *Reservoir* tab of the Builder. Other properties, like the fluid composition, will be defined in the next section.

Fluid Modelling

The fluid model can be described inside Builder, or it can be imported. In our case, we created a fluid model based on a given recombined composition (10 pseudo components), the saturation pressure and two available lab tests: Differential Liberation (DL) and Constant Composition Expansion (CCE). Table 2 shows a summary of the PVT properties. The starting composition is shown in Table 3.

Table 2: Summary of PVT properties

		SI		*Field Units*
Reservoir Temperature (T_r)	70	C	158	F
Saturation Pressure (p_b)	55	kg/cm2	924.5	psi
R_s	52.5	m3/m3	294.76	scf/bbl
B_o	1.21	m3/m3	1.21	res bbl/STB
ρ_l	751	kg/m3		
ρ_l @ s.c.	845	kg/m3	36	API
μ @r.c	1	cp		

Table 3: Initial fluid composition

Component / Pseudo component	*Z_i(%)*	*w_i (%)*	*M_w*	*γ*
CO2	0	0		
C1	25.817	2.008		
C2	10.745	1.566		
C3	7.767	1.66		
C4	5.124	1.444		
C5	2.518	0.881		
C6	3.12	1.271		
C9	4.07	2.388		
C14	15.105	13.916		
C19	25.732	74.863	600	0.933
SUM	**99.998**	**99.997**		

This section will provide a brief, but clear methodology to create a representative fluid model for our compositional simulation. A more in depth guide to using WINPROP may be found at CMG's website, or within the guides contained in the CMG Simulation suite.

The general workflow is as follows:

1. Define the units of the fluid model (SI)
2. Define an Equation of State (EOS). In this case we will use Peng Robinson (1978)
3. Capture the composition.
4. Capture the saturation pressure and the available lab tests. DL and CCE are available for our simulation.
5. Perform regression on the parameters that are uncertain, and try to fix or increase the weighting on those that are well known (i.e. Saturation pressure)
6. Once the calculated properties of the fluid match the lab tests satisfactorily, export the model to GEM.

As for the first step and second step, the first screen of WINPROP will help us setup those the units and the EOS. (Fig. 13)

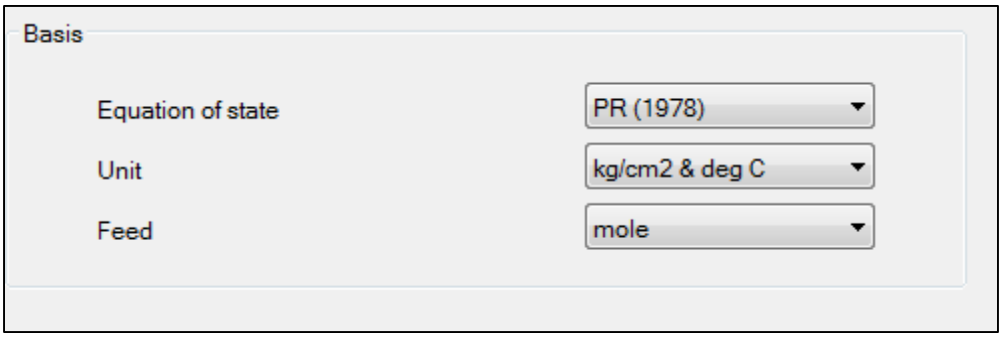

Figure 13: Unit and EOS definition.

While capturing the composition (Fig. 14) it is advisable to add a small amount of CO2 into the original fluid. This will allow for easier calculations when calculating the interaction of the primary (original) and secondary (injection) fluids. Propane (44.096 lb /

lb mol) is of about the same molecular weight of CO_2 (44.0095 lb / lb mol), therefore, we may subtract the amount that we will add to for CO_2.

Component	Primary	Secondary
CO2	0.001	1
CH4	0.25817	0
C2H6	0.10745	0
C3H8	0.07669	0
NC4	0.05124	0
NC5	0.02518	0
FC6	0.0312	0
FC9	0.0407	0
FC14	0.15105	0
C19+	0.25732	0
Sum	1	1

Figure 14: Fluid composition. *Primary* refers to the reservoir fluid. *Secondary* to the injection fluid (CO_2)

The saturation pressure and the lab tests are captured inside a regression block (Fig. 15). By doing so, and running the regression subroutine, we will tune our EOS. As a general guideline, the volumetric properties of the heavier fractions or the pseudo components should be tuned first, as they have the highest uncertainty. The properties of the plus fraction (in this case C19+) are the ones with more uncertainty (McCain, 2015). While matching the lab tests, we would recommend to vary one or two parameters at a time and, when that does not yield satisfactory results, we may group similar or related properties and run the regression. Weighting factors will also play a key role in trying to match the tests. Finally, it is advisable that we match the viscosity at the end of the tuning process. We recommend doing so by increasing the weighting factor on viscosity data and

running the regression several times, allowing for a an improvement on the viscosity match without affecting other fluid properties. Fig. 16 and 17 are screenshots of the DL and CCE blocks.

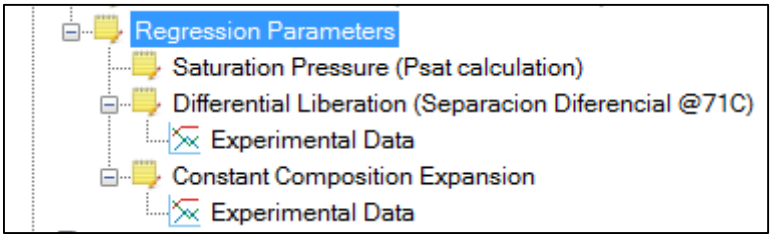

Figure 15: Fluid regression block

Pressure Levels | Consistency Checks | Feed/K values/Output level/Stability test level/Standard conditions

Comments: Separacion Diferencial @71C

Temperature (deg C): 71

Scale ROV and GOR to oil shrinkage and cum. gas released relative to bubble point

Improve saturation pressure estimate

Copy Consistency Checks Table Contents

No. of pres. levels (the row No. 0 is reserved for sat. pres): 10

Tools

No.	Pressure (kg/cm2)	Oil FVF (rm3/sm3)	GOR (std m3/std m3)	Oil SG	Gas Z Factor	Gas FVF (rm3/sm3)	Gas SG (Air = 1)	Oil Viscosity (cp)
	Weight	1	1	1	1	1	1	5
0	55.5	1.1923	50.3	0.7609				0.9998
1	400.5	1.1454	50.3	0.792				1.4201
2	350	1.1506	50.3	0.7885				1.3998
3	297	1.1566	50.3	0.7844				1.3503
4	251	1.1621	50.3	0.7806				1.2999
5	202.5	1.1686	50.3	0.7763				1.2503
6	150	1.1767	50.3	0.771				1.2001
7	108	1.1831	50.3	0.7668				1.0998
8	38	1.1642	40.1	0.7707		0.0239	0.8006	1.1
9	26	1.1423	31.7	0.7785		0.0418	0.7955	1.18
10	16	1.1252	25.1	0.7843		0.0663	0.8498	1.2999

Figure 16: DL test data. A weighting factor of 5 in oil viscosity is set for viscosity matching purposes.

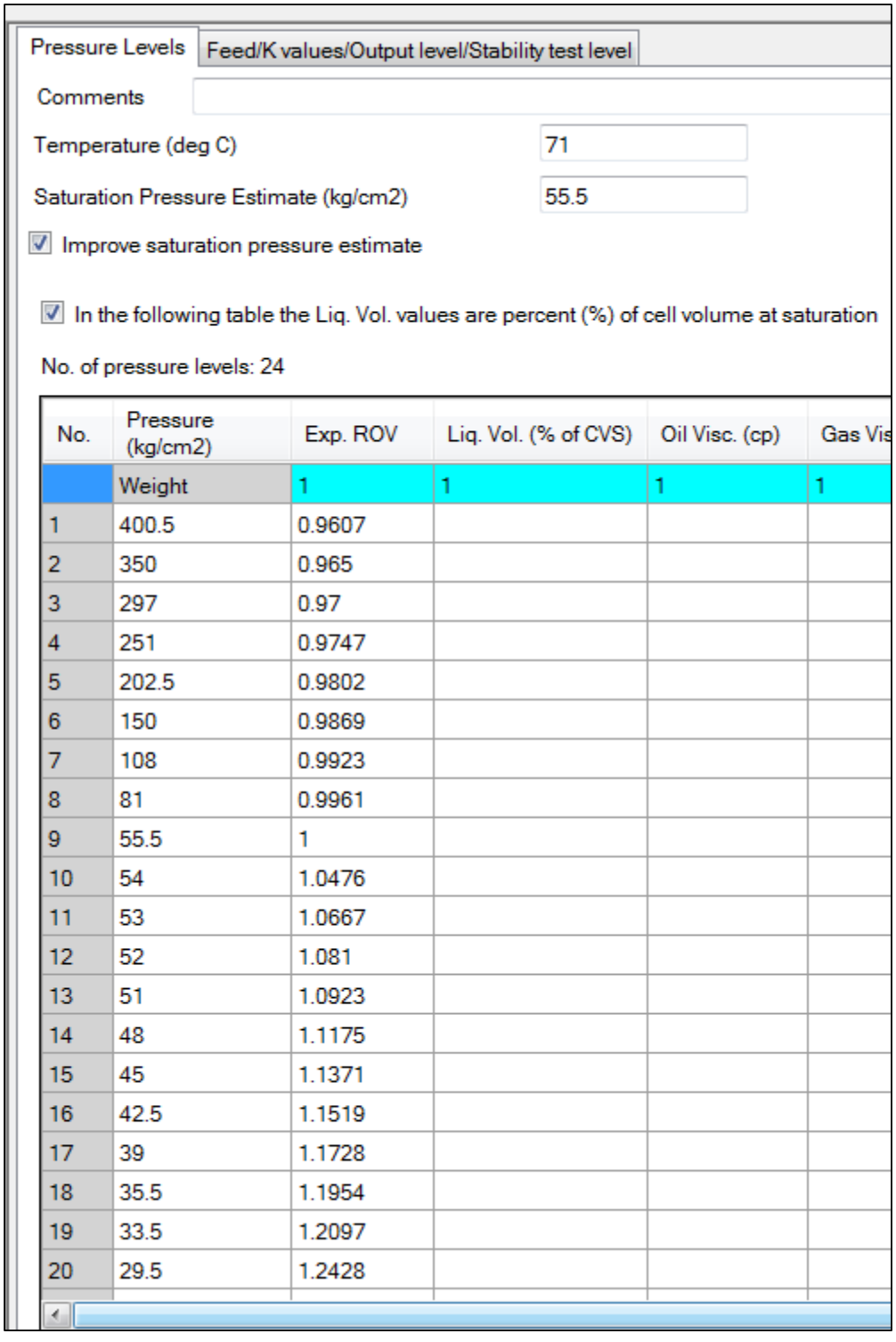

Pressure Levels | Feed/K values/Output level/Stability test level

Comments

Temperature (deg C) 71

Saturation Pressure Estimate (kg/cm2) 55.5

☑ Improve saturation pressure estimate

☑ In the following table the Liq. Vol. values are percent (%) of cell volume at saturation

No. of pressure levels: 24

No.	Pressure (kg/cm2)	Exp. ROV	Liq. Vol. (% of CVS)	Oil Visc. (cp)	Gas Vis
	Weight	1	1	1	1
1	400.5	0.9607			
2	350	0.965			
3	297	0.97			
4	251	0.9747			
5	202.5	0.9802			
6	150	0.9869			
7	108	0.9923			
8	81	0.9961			
9	55.5	1			
10	54	1.0476			
11	53	1.0667			
12	52	1.081			
13	51	1.0923			
14	48	1.1175			
15	45	1.1371			
16	42.5	1.1519			
17	39	1.1728			
18	35.5	1.1954			
19	33.5	1.2097			
20	29.5	1.2428			

Figure 17: CCE test data.

After performing the regressions, calculated fluid properties should closely resemble to those of the lab tests. In this case, Fig. 18,19,20,21 and 22 show our measured versus calculated behavior. The continuous line represents the fluid model calculations, while the dots represent the experimental data.

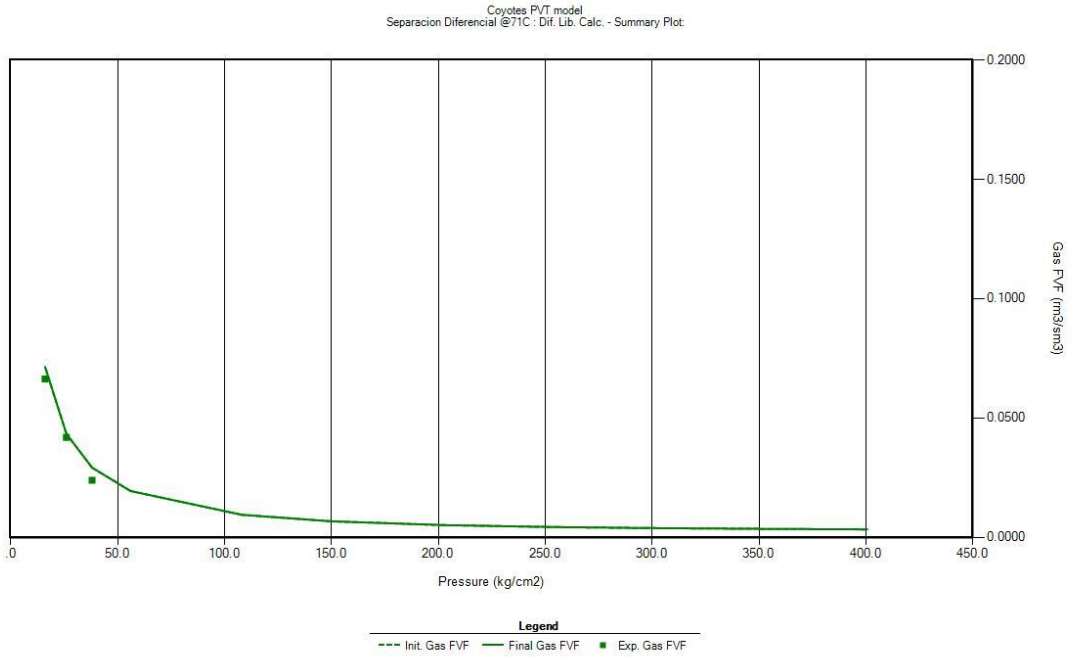

Figure 18: Gas formation volume factor (Gas FVF)

As shown in the figures, very good matches were obtained for the Gas FVF, Oil viscosity, GOR, Gas SG and Oil SG. A representative match was obtained for the Relative volume (CCE) and the ROV.

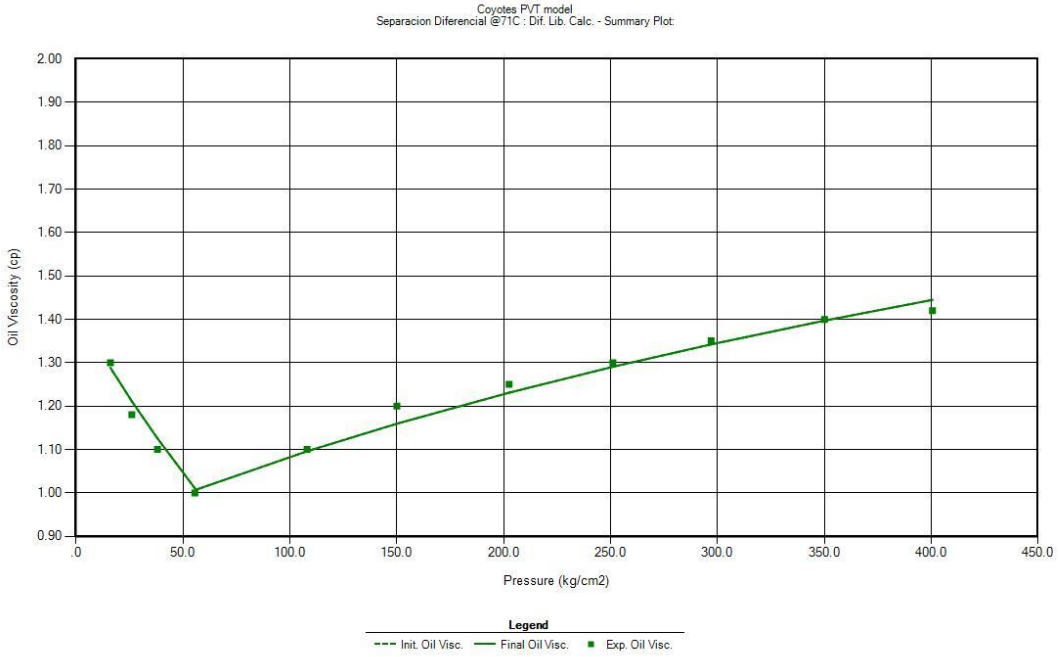

Figure 19: Oil viscosity

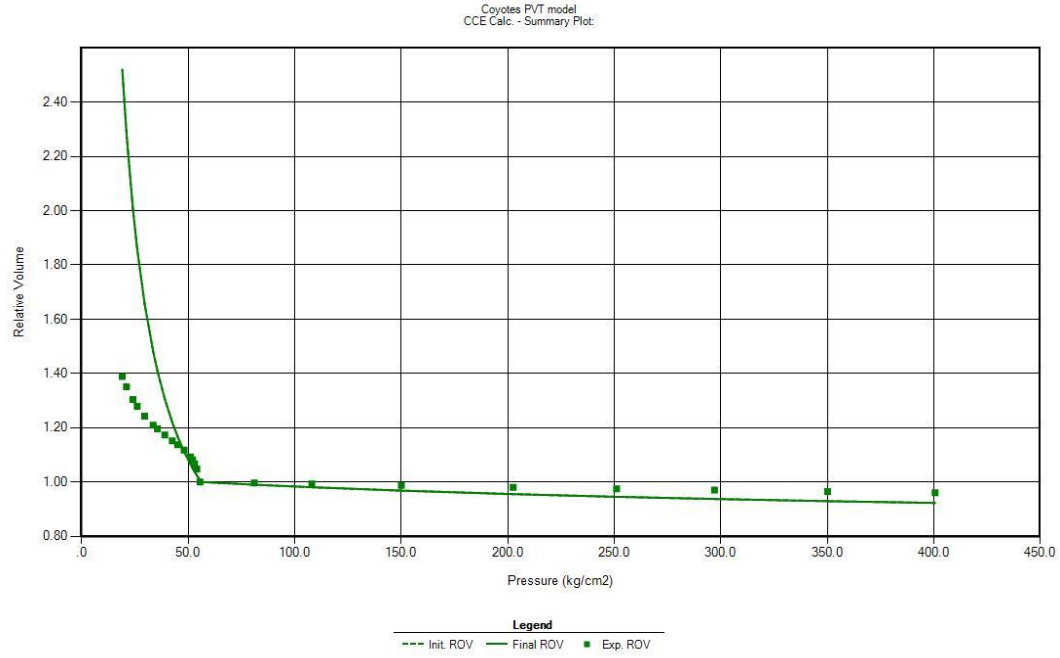

Figure 20: Relative volume from constant composition expansion (CCE)

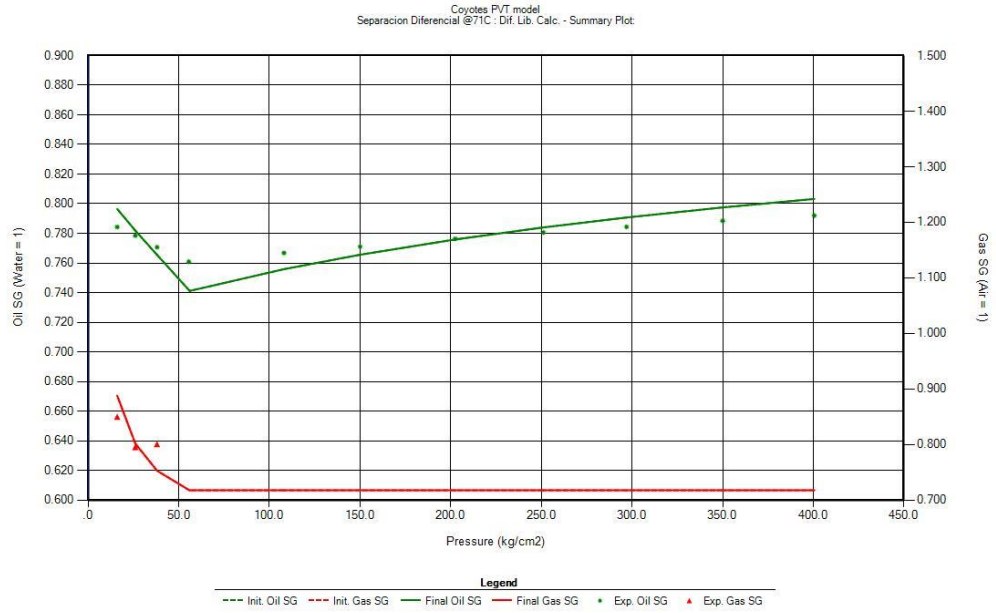

Figure 21: Oil and gas specific gravities. Upper line corresponds to oil and the bottom line to gas.

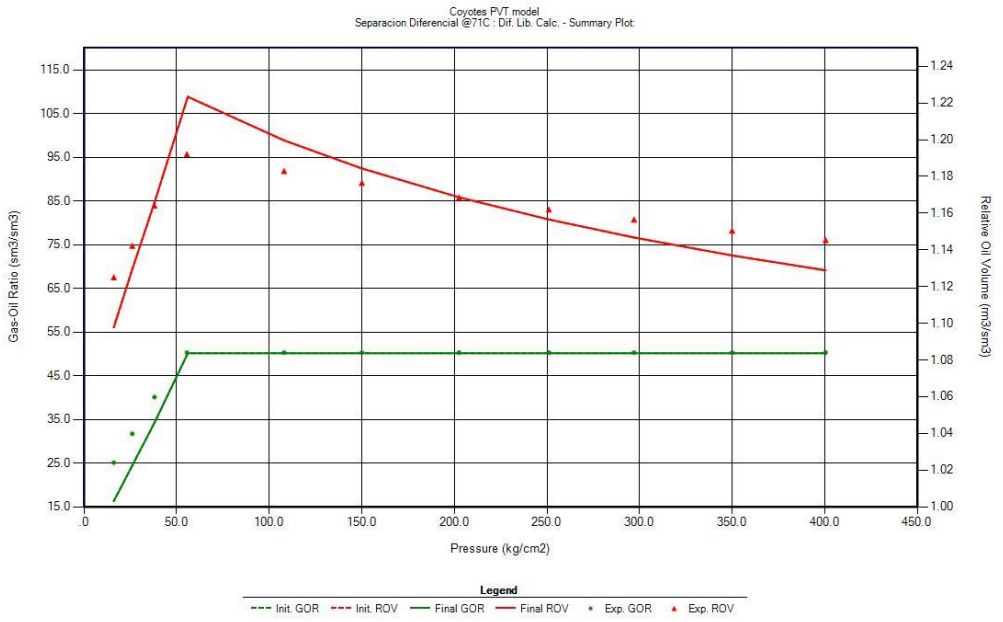

Figure 22: Relative oil volume (ROV) and Gas-Oil Ratio (GOR). Upper line corresponds to ROV and bottom line to GOR.

After obtaining a representative fluid model in WINPROP, this should be exported for later use in GEM.

Due to optimization goals, an alternative fluid model was prepared reducing the number of pseudo-components, but it was not used. The grouping was made by selecting those similar components in terms of the M_w, but most importantly, based on the idea that no significant changes should occur in the phase envelope at the saturation pressure and reservoir temperature. Fig. 23 corresponds to the 10 pseudo-components model and Fig. 24 to an optimized 7 pseudo-components. Additional attempts were made to reduce the number of pseudo-components to 6, but the saturation pressure condition could not be achieved.

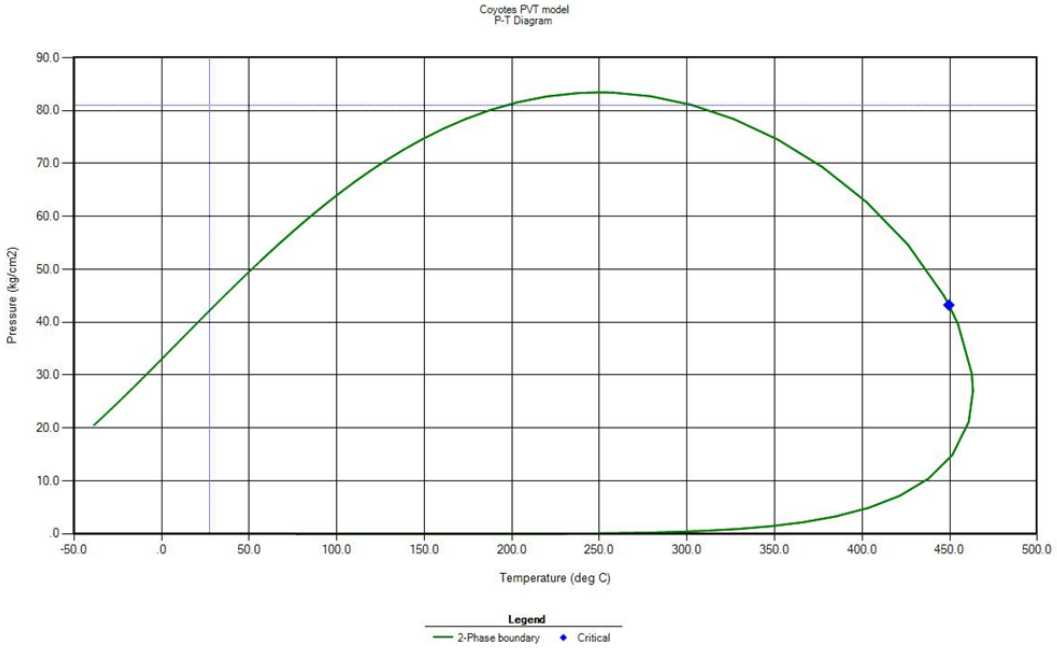

Figure 23: Phase envelope, 10 pseudo-components.

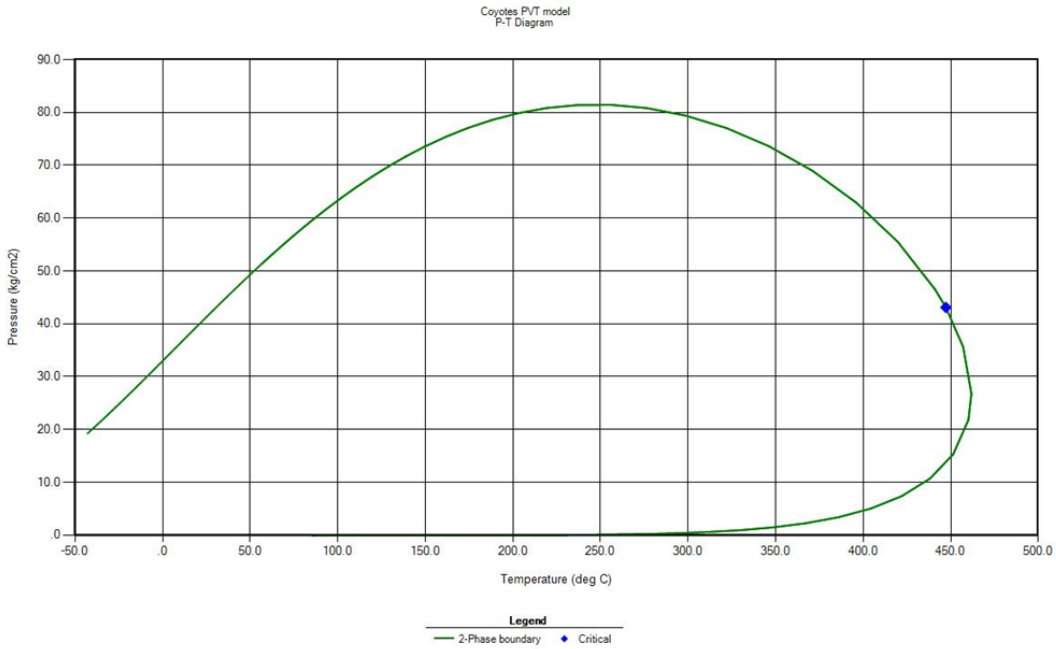

Figure 24: Phase envelope, 7 pseudo-components.

Once that we create the fluid model, importing it into Builder is not complicated. Under the *Components* tab, we will click *Model* and select *Import*, then we will select our *.gem* file and click *open*. The EOS, reservoir temperature, viscosity correlation, and the composition will automatically update. Additionally, the composition will be updated under the *Reservoir* tab.

Rock-Fluid Interaction

Permeability data was measured by PEMEX from cores of correlation wells. This poses a certain degree of uncertainty, but it is the best available data. Core plugs were tested, permeability and porosity were measured.

From the petrophysical analysis, a set of relative permeability curves were obtained. Fig. 25 is the relative permeability of oil (k_{ro}) and water (k_{rw}) as a function of the water saturation (S_w) Fig. 26 is the relative permeability of oil (k_{ro}) and gas (k_{rg}) as a function of gas saturation (S_g).

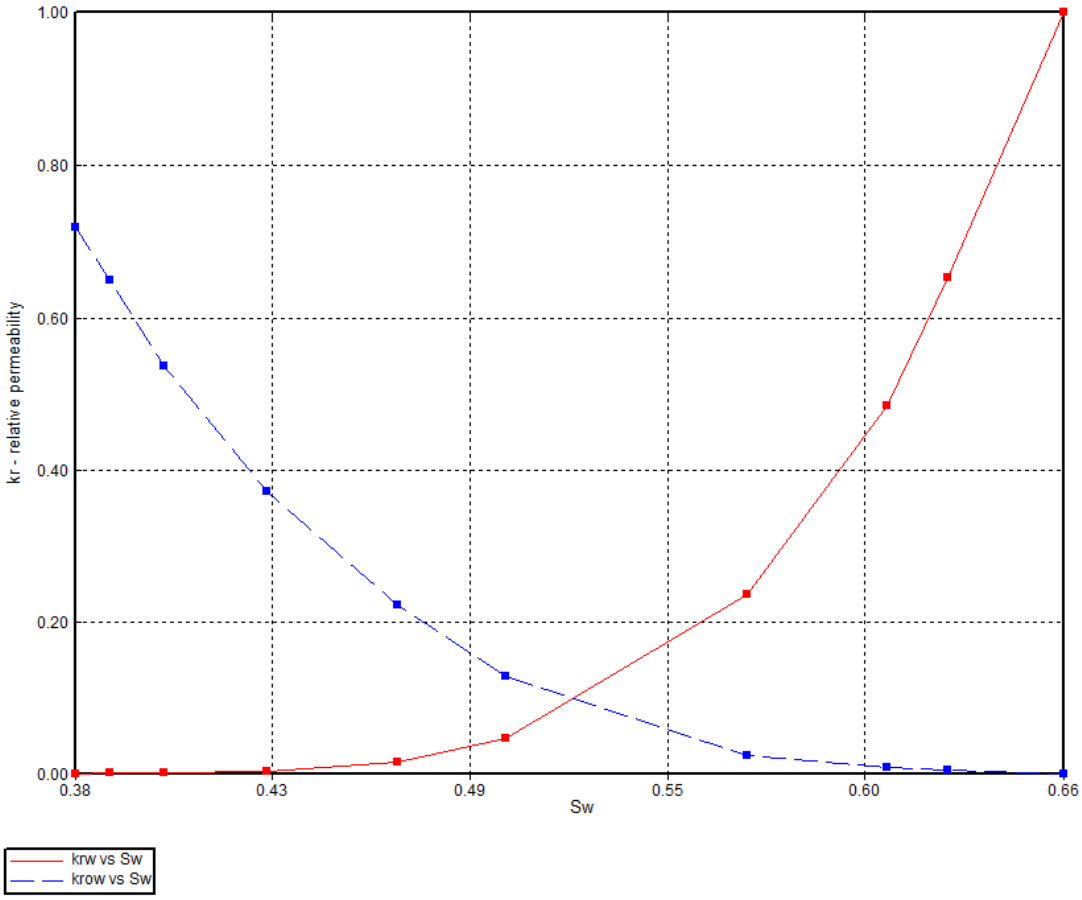

Figure 25: k_{ro} and k_{rw} as a function of Sw

Builder provides an easy interface to input the permeability data. First a *Rocktype* should be created, and then the permeability for the Water-Oil Table and Liquid-Gas Table should be entered. As a result, Fig. 25 and 26 will be created. An additional plot, Fig. 27

is created based on the two tables and serves as a visual guide of the permeability functions.

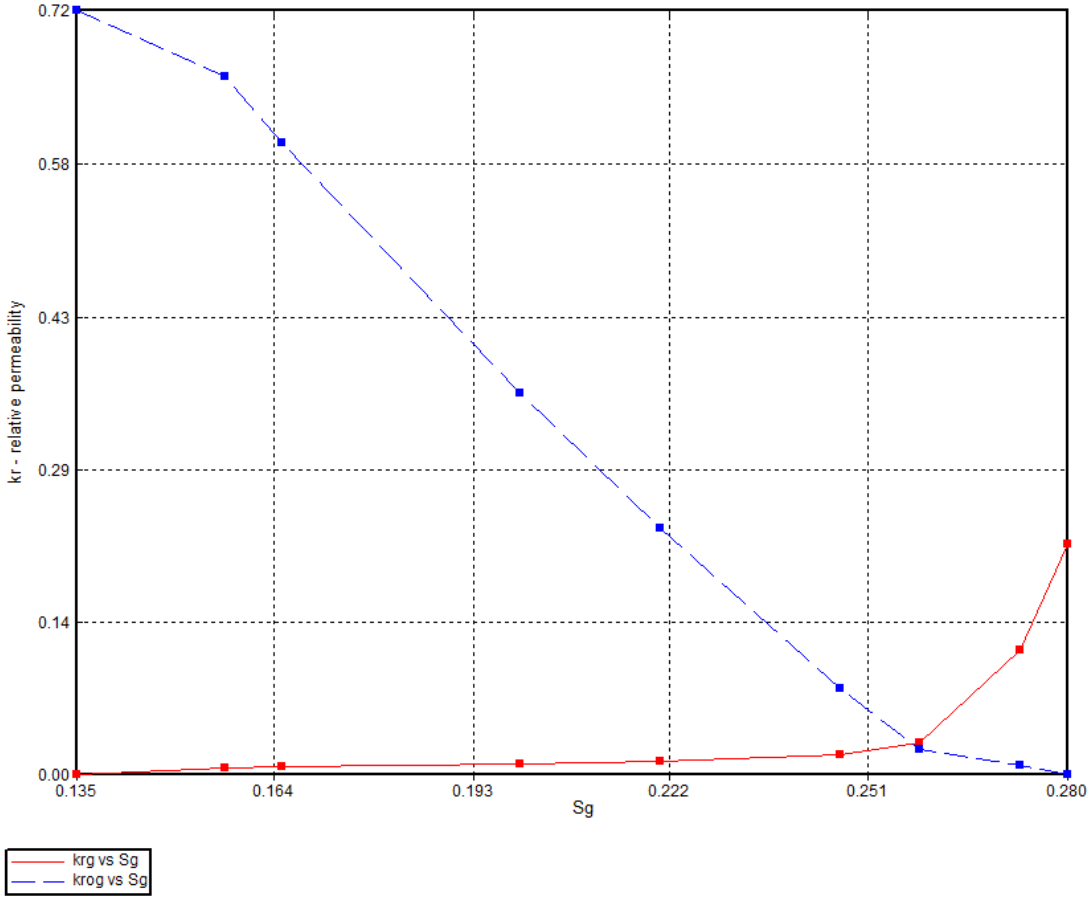

Figure 26: k_{ro} and k_{rg} as a function of Sg

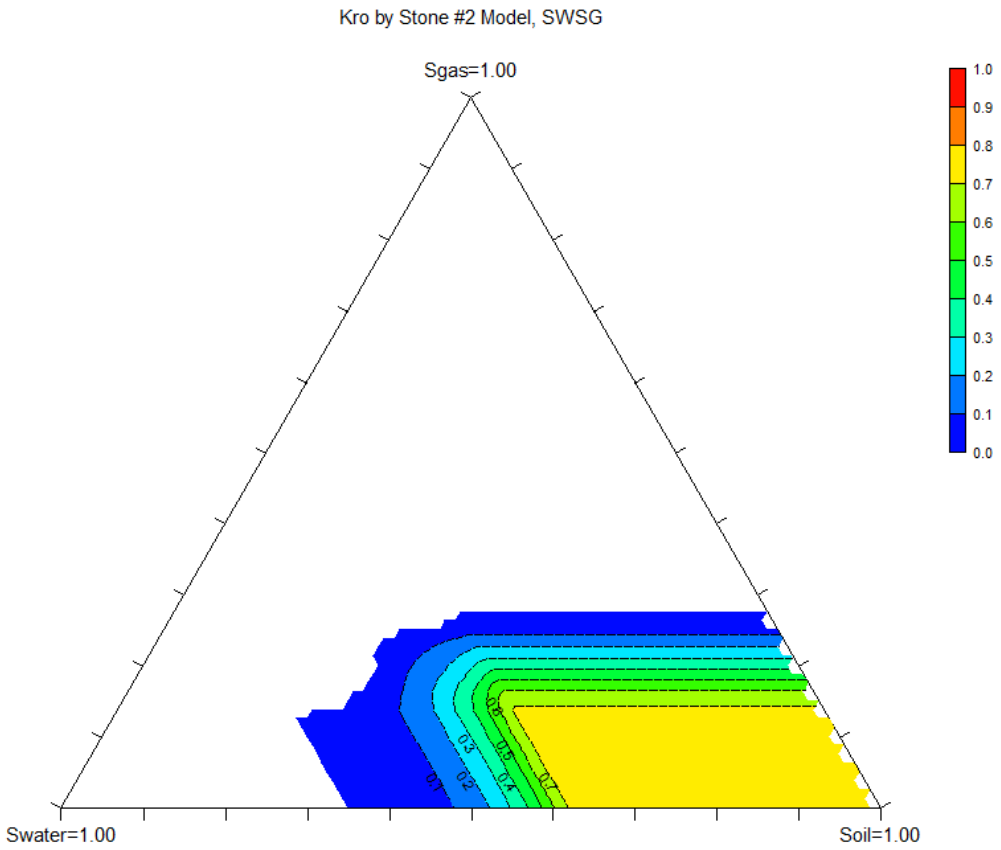

Figure 27: Relative oil permeability as a function of fluid saturation.

Initial Conditions

In this section we define the initial reservoir pressure and reference depth. Additionally, the water oil contact (if any) and whether there is free gas or not. For our study case, the initial reservoir pressure is 8951.5 kPa (1298 psi) and the datum is fixed at 852 m (2795 ft). There is no free gas nor an aquifer.

Numerical

Numerical controls are set to default. Minimum and maximum time step sizes are defined here, along with other numerical controls like the number of Newton-Raphson iterations and the maximum number of linear solver iterations. No changes were made before the optimization part of this study.

Wells, Completions and Production Data.

One of the main objectives during the pilot test was to prove hydraulic communication between wells perforated on the same sand body. Due to this, the seven wells crossed three stratigraphic sequences of the Chicontepec formation, but were only perforated in the most superficial one. Additionally, six out of seven wells were hydraulically fractured, the injector included. A general schematic of the inverted seven spot arrangement is found on Fig. 28.

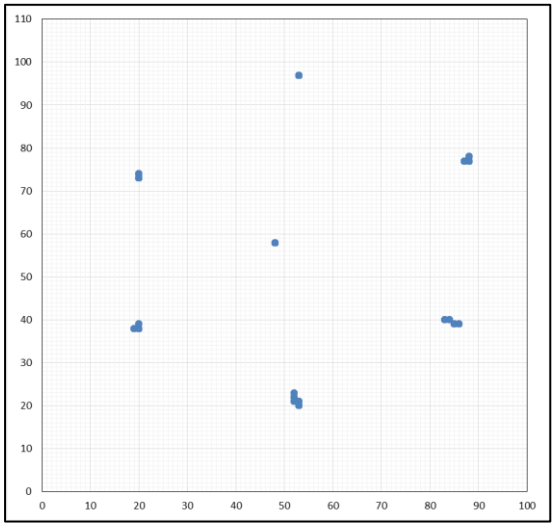

Figure 28: Top view of the well arrangement in the numerical model. Each blue point represents a pair of (x,y) nodes, for each plane that the well crosses.

In Builder, the *Wells & Recurrent* section handles well trajectory, completion, production data and date keywords.

The trajectory as well as the perforations are to be set under the *Well > Well Completions (PERF) > Perforations.* There are several alternatives for introducing the data into the numerical model (as found on the Builder's user guide). We found that an easy alternative is to create the write down the blocks that will correspond to the trajectory, i.e. 31 15 1 to 31 15 5 (which stands for 31 in *x* direction, 15 in *y* direction and 1-5 in *z* direction). Then, activate or deactivate the block depending on the perforations. Fig. 29 shows a schematic of the final well disposition in the optimized model.

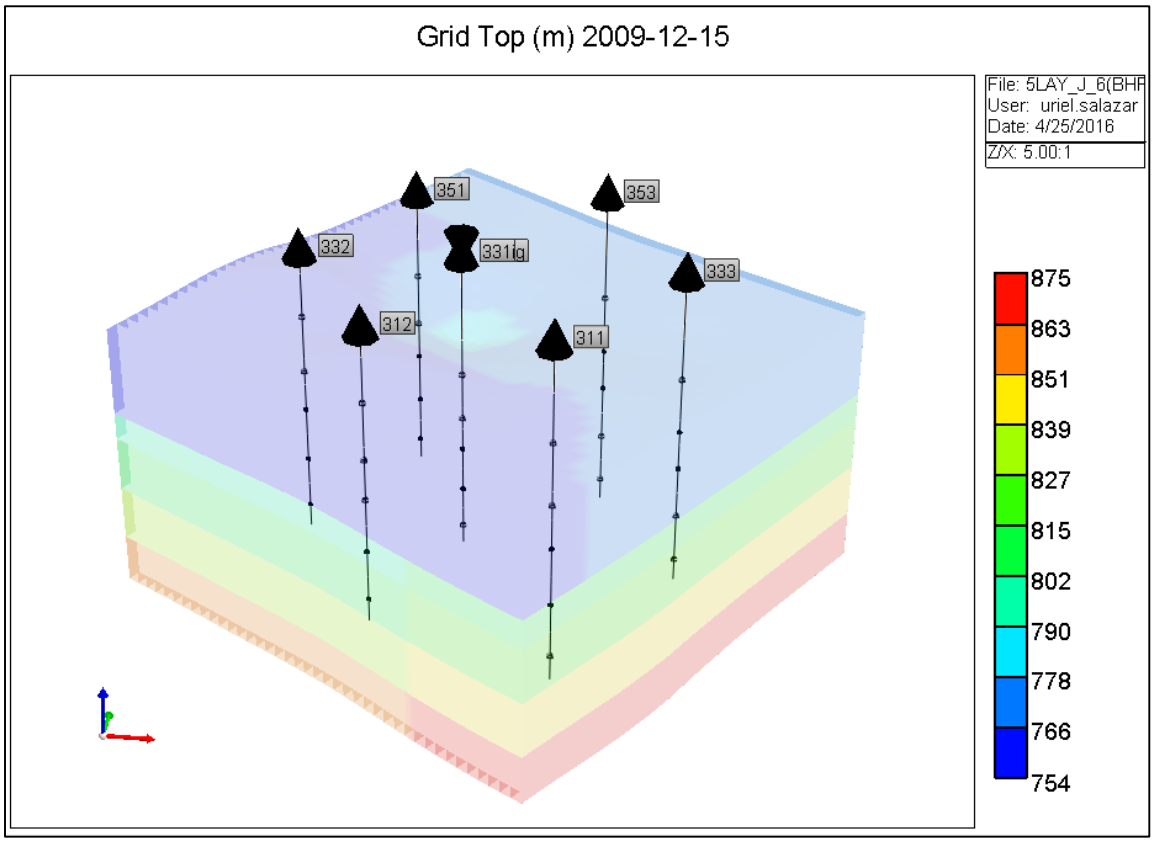

Figure 29: Well disposition and perforations in the final, optimized model.

As for hydraulic fractures, they are set explicitly. All but the offset well, 332, are hydraulically fractured, with fracture planes oriented N (27° ± 3) E. This suggests an orientation of the fracture planes for the wells 312, 352 and 331 (gas injector). Table 4 summarizes the fracture design information. Additional work on the fracture setup was done during the optimization section of this work.

Table 4: Hydraulic fracture design summary.

Well	x_f *[m]*	h_f *[m]*	w_f *[in]*	C_f *[md-m]*	C_f *[md-ft]*
312	123.9	35.3	0.54	2382	7814
351	134.1	45.8	0.6	1622	5322
331 (inj)	118.8	42.1	0.62	1698	5571
311	122.1	42.8	0.56	1844	6051
353	152.3	27.1	0.59	2134	7000
333	40.6	17.8	0.52	1128	3702
332	--	--	--	--	--

Production data constitutes a source of continuous information for this pilot test. Tables 5, 6, 7 and 8 summarize monthly production data. The dates are in DD/MM/YYYY format. All of this data went into builder under the *Well > Import Production/Injection Data*. In this sense, the data needs to be preconditioned into a *.prd* file for builder to access it. Production data, by well and for each reference date is created and written into a word processor, then saved it with a *.prd* extension.

Table 5: Monthly oil production

Qo (b/d)	311	312	**331**	332	333	351	353	Total
15/12/2009		16.5	5.1	10.1	69.6			101.3
15/01/2010	26.1	56.8	9.1	46.9	164.4	22.9	26.1	352.2
15/02/2010	17.8	47.6	5.9	41.6	148.7	23.8	17.8	303.4
15/03/2010	19.8	52.7	19.3	46.1	164.8	26.4	19.8	348.8
15/04/2010	19.1	50.8	19.1	44.4	158.5	25.5	19.1	336.6
15/05/2010	23.1	30.2	15.4	21.6	163.2	30.3	19.6	303.4
15/06/2010	24.9	18.7	12.9	13.7	158.6	32	17.4	278.3
15/07/2010	13.1	11.6		11.9	155.6	11.9	3.2	207.3
15/08/2010	6.1	6.7		11.8	161.4	8.3	8.6	202.8
15/09/2010	14.8	6.6		12.5	151.9	8.1	12.2	206.2
15/10/2010	13.4	3.5		12.8	134.4	8.3	6.4	178.8
15/11/2010	12.9			12.3	129.3	7.3	6.2	168
15/12/2010	12.2			11.9	84.6	5.9	3.1	117.6
15/01/2011	12.4			8.2	68.1	5.1		93.7
Np (b)	**6,471**	**9,051**	**2,604**	**9,174**	**57,393**	**6,474**	**4,785**	**95,952**

Table 6: Monthly gas production

Qg (scf/d)	311	312	**331**	332	333	351	353	Total
15/12/2009		9,268	2,851	5,703	39,129			56,953
15/01/2010	14,839	32,293	5,167	26,648	93,508	13,050	14,839	200,347
15/02/2010	10,116	26,977	3,372	23,605	84,305	13,488	10,116	171,982
15/03/2010	11,135	29,711	10,900	25,991	92,842	14,855	11,135	196,573
15/04/2010	10,794	28,622	10,794	25,029	89,341	14,393	10,794	189,770
15/05/2010	13,040	17,041	8,677	12,153	92,042	17,079	11,045	171,079
15/06/2010	14,526	20,788	14,843	7,604	92,818	18,575	9,852	179,010
15/07/2010	8,580	20,910		8,649	111,530	6,572	1,453	157,694
15/08/2010	11,795	15,727		14,385	123,342	4,049	6,368	175,667
15/09/2010	28,723	22,831		15,854	121,710	3,963	10,413	203,494
15/10/2010	24,677	18,412		16,451	111,043	4,113	8,226	182,922
15/11/2010	23,002			15,338	103,519	3,696	7,663	153,219
15/12/2010	20,953			12,827	76,243	3,207	3,462	116,691
15/01/2011	23,255			10,300	73,087	3,360		110,002
Gp (Mscf)	**6463.05**	**7277.4**	**1698.12**	**6616.11**	**39133.77**	**3612**	**3160.98**	**67962.09**

Table 7: Monthly water production

Qw (b/d)	311	312	**331**	332	333	351	353	Total
15/12/2009		0	0	0	0			0
15/01/2010	8.3	29.1	17.4	5.8	0	5.8	8.3	74.7
15/02/2010	17	28.3	17	5.7	0	5.7	17	90.5
15/03/2010	18.8	31.4	6.7	6.3	0	6.3	18.8	88.4
15/04/2010	18.2	30.2	6.1	6.1	0	6.1	18.2	84.8
15/05/2010	11.7	10.1	2.2	6.1	0	2.2	18.2	50.5
15/06/2010	1.8	0.1	0	1.4	0	0	2.5	5.8
15/07/2010	0.8	0.2		1.3	0	0	0.4	2.8
15/08/2010	0.3	0.3		1.3	0	1.3	3.6	6.9
15/09/2010	1.3	0.3		0.9	0	1.3	3.7	7.6
15/10/2010	3.9	0.2		1.1	0	1.6	1.9	8.7
15/11/2010	4.1			1.1	0	1.5	1.9	8.7
15/12/2010	4.8			1.3	0	1.5	1.2	8.8
15/01/2011	4.9			0.1	0	2.4		7.4
Wp (b)	**2,877**	**3,906**	**1,482**	**1,155**	**0**	**1,071**	**2,871**	**13,368**

Table 8: Monthly GOR

GOR (scf/STB)	311	312	**331**	332	333	351	353
15/12/2009		561.697	559.0196	564.6535	562.1983		
15/01/2010	568.5441	568.5387	567.8022	568.1876	568.7835	569.869	568.5441
15/02/2010	568.3146	566.7437	571.5254	567.4279	566.9469	566.7227	568.3146
15/03/2010	562.3737	563.7761	564.7668	563.7961	563.3617	562.6894	562.3737
15/04/2010	565.1309	563.4252	565.1309	563.7162	563.6656	564.4314	565.1309
15/05/2010	564.5022	564.2715	563.4416	562.6389	563.9828	563.6634	563.5204
15/06/2010	583.3735	1111.658	1150.62	555.0365	585.2333	580.4688	566.2069
15/07/2010	654.9618	1802.586		726.8067	716.7738	552.2689	454.0625
15/08/2010	1933.607	2347.313		1219.068	764.2007	487.8313	740.4651
15/09/2010	1940.743	3459.242		1268.32	801.2508	489.2593	853.5246
15/10/2010	1841.567	5260.571		1285.234	826.2128	495.5422	1285.313
15/11/2010	1783.101			1246.992	800.611	506.3014	1235.968
15/12/2010	1717.459			1077.899	901.2175	543.5593	1116.774
15/01/2011	1875.403			1256.098	1073.231	658.8235	

As for injection data, Fig. 30 shows the pressure and injection data that went into the model. Pressure data is fairly continuous, except for those periods where no data was recorded.

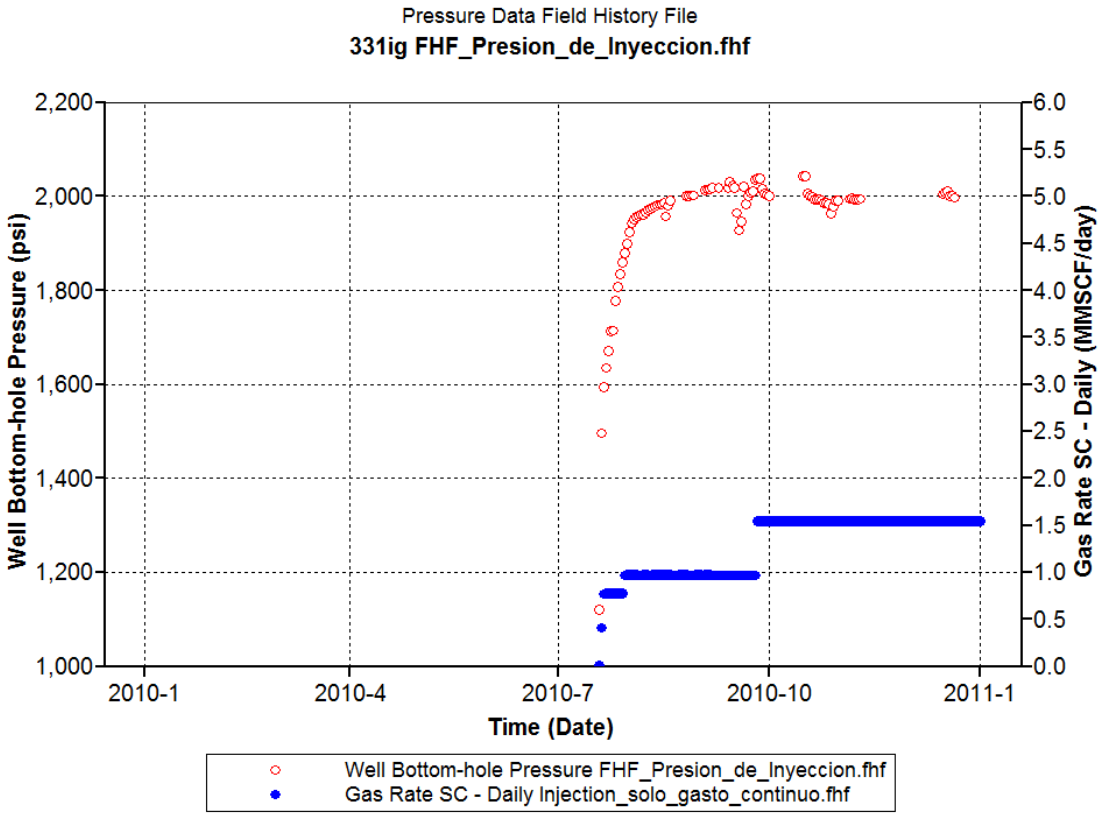

Figure 30: Injection data for well 331ig (CO_2 injector)

Once all of the data was captured, we performed a first simulation run to check for inconsistencies or errors. No problems were found at this stage, except for the large running times.

The following section will discuss some performance issues found during the first simulations and the optimization work to reduce the computing time.

Optimization

While theory exists regarding the ideal time step sizes for different scenarios, we decided to approach the problem from a trial-error mindset, focusing on three main guidelines:

1. Creating a faster, explicit way to represent the fracture
2. Reducing the number of cells of the reservoir model, which at first consisted on 64,000 cells
3. Modifying the numerical controls

At first, the geometrical properties of the hydraulic fractures were poured into the numerical model, explicitly representing it by the use of grid refinement and a permeability value for the fracture. This created a big contrast of permeabilities from the hydraulic fractures to that of the neighbor blocks, introducing several convergence errors. The problem became more obvious as CO_2 injection started, with the simulator getting messages, such as: "--- *Repeat time step: program failed to converge*" and running times notably increasing, taking up to 10 hours to run the base case.

Then, in order to allow for a more manageable contrast of permeabilities, we decided to represent the fracture without the use of grid refinement, but rather by creating a sort of "fractured area" with thickness of the size of a grid block, thus lowering the permeabilities but keeping the conductivities constant. Since near fracture effects are of no interest to this study, this seemed logical and numerically consistent. We compared the results from the base case to that of the optimized fracture case obtaining identical results, but with 3 times lower computing times.

Secondly, given the reservoir's net thickness, averaging 6.8 m (22 ft), we decided that the amount of refinement obtained from 40 layers did not justify the running time. Therefore we decided to create a more manageable model of no more than 8 layers. Most commercial simulators make use of upscaling algorithms, and CMG's not different. The grouping of the layers, however, was made manually and not automatically setup. From a trial and error standpoint we decided to create 8, 7, 6, 5 and 4 layer models and compare it to the base case results. No significant loss of accuracy was obtained with 5 layers and we decided to use that as our optimized simulation model.

Finally, we modified a few numerical controls to allow for more flexibility. Given the interactions between the well and the hydraulic fracture, and the CO_2 injection in a hydraulically fractured well, we reduced the time step size (both maximum and minimum) and ran the simulation, successfully reducing the computing time. A list of all the modified numerical controls may be found in Table 9.

Table 9: List of modified numerical controls

Numerical control	*Default value*	*Modified value*
Maximum time step size	365 day	15 day
Minimum time step size	1e-005 day	1e-007 day
First time step size after well change	0.01 day	0.005 day
Normal pressure variation per time step	1000 kPa	6000 kPa
Maximum Newton iterations	10	15
Linear solver iterations	80	200
Linear solver orthogonalizations	40	200

History Matching

As defined by Ertekin, *et al.* (2001): "manual history matching involves running the simulation model for the historical period and compare it to the known field behavior. Then the model may be adjusted by the reservoir engineer in an effort to match the observed behavior. Selecting which data to adjust requires knowledge of the field under study, as well as engineering judgment and reservoir engineering experience."

Additionally, the reliability of data plays a key role. Table 10 summarizes the available data for this study.

Table 10: Summary of available data

Data	*Source*	*Frequency*	*Quality*
Injector BHP	Permanent downhole gauge	Hourly, with three big data gaps	Excellent
CO_2 injection rates	Surface pumping rates	Daily	Excellent
Well liquid rates	Occasional measurements	Daily (prorated)	Regular
Well gas rates	Occasional measurements	Daily (prorated)	Bad
Producers BHP	Echometers	Daily for one weeks	Regular
Pre-flooding compositional analysis	Recombined surface sample	One, before flooding	Good
During-flooding compositional analysis	Surface oil sample	Two after early breakthrough	Bad
Permeability	Old core plugs from similar wells	----	Good data, but referential
Hydraulic fractures	Designs and Post-job reports	----	Good

As observed from Table 10, the best quality data is that of the injector well, followed by the hydraulic fracture data and ending with somewhat reliable production data. It is important to note that production data is good, but the pad arrangement did not allowed for the continuous measurement of the wells, therefore relying on intermittent individual measurements to adjust the pad production data.

Another interesting observation falls on the permeability data. The analyzed cores correspond to other similar wells, cut during previous development attempts of the Chicontepec field. These cores were previously analyzed and plugs were cut several years before this study. We consider that the best sections of the core were cut, as they were interested in the higher permeability areas. Preservation issues are also suspected. As a consequence, the permeability model underestimates the actual permeability, topping it at 0.7 [md] while the petrophysical analysis show that a few sections would reach permeabilities as high as 6.0 [md]. Taking into account these premises, and those from a previous work by Cinco, Salazar, *et al.* (2011), we decided to prove that permeability is indeed higher by two strategies: first regression analysis and then numerical simulation.

In Cinco, Salazar, *et al.* (2011), as part of a previous Chicontepec study, we observed that some Chicontepec well tests suggest linear, bilinear and sometimes trilinear behavior. These were clear signals of channel-like reservoir geometries and high heterogeneity. Based on that premise, and the calculated channel geometries obtained in 2011, we input the data along with reservoir parameters into the linear flow solution for the only non-fractured well, Well 332. The results of the match are shown in Fig. 31.

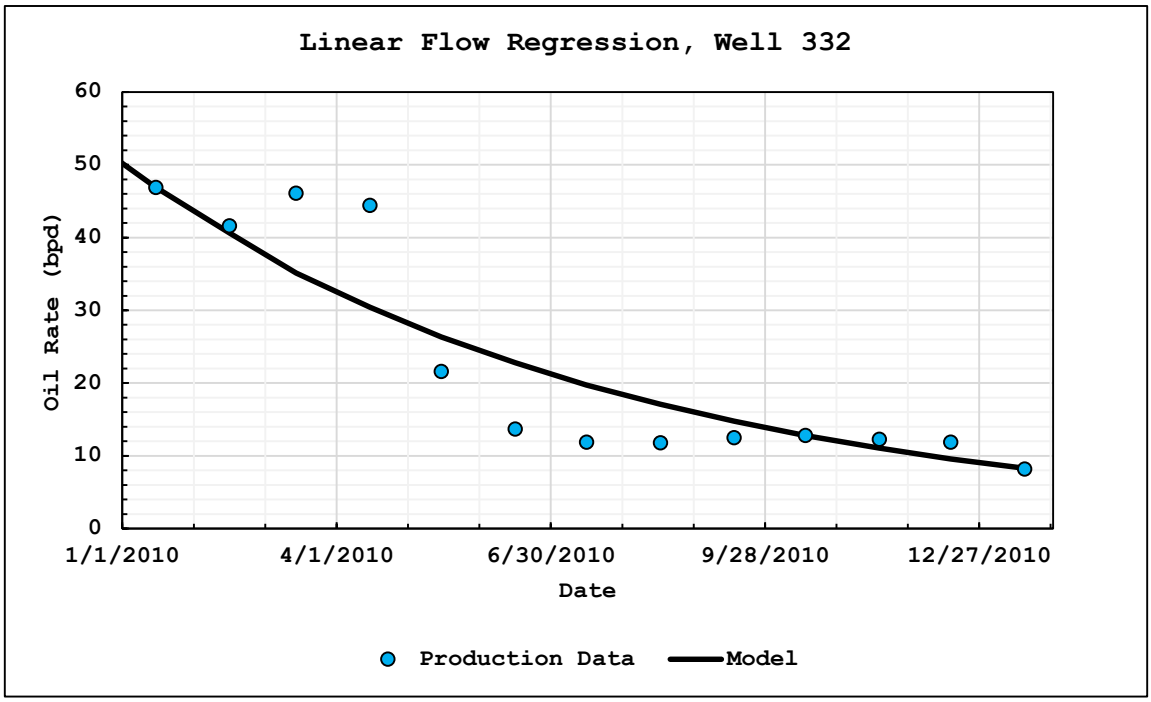

Figure 31: Linear flow regression for well 332.

While not perfect a perfect match, perhaps due to the quality of the production data, the model suggests an average permeability, *k*, of 5.2 [md] with a regression error of 6.8 %. This result is bigger than the limited permeability model and agrees with the higher permeability samples of the petrophysical analysis. Now, before liberally fixing new permeabilities, several scenarios were run on the optimized model for different permeability multipliers. The injector well data was honored and considered the most accurate and reliable set of information. The base case is shown Fig. 32. The injection BHP is clearly out of range for the base case. The latter confirms that k is underestimated.

For all the scenarios that we ran, we obtained a somewhat good match in early behavior, but late pressure data didn't match at all with an acceptable permeability modifier. Also, early breakthrough have not occurred in the simulation cases.

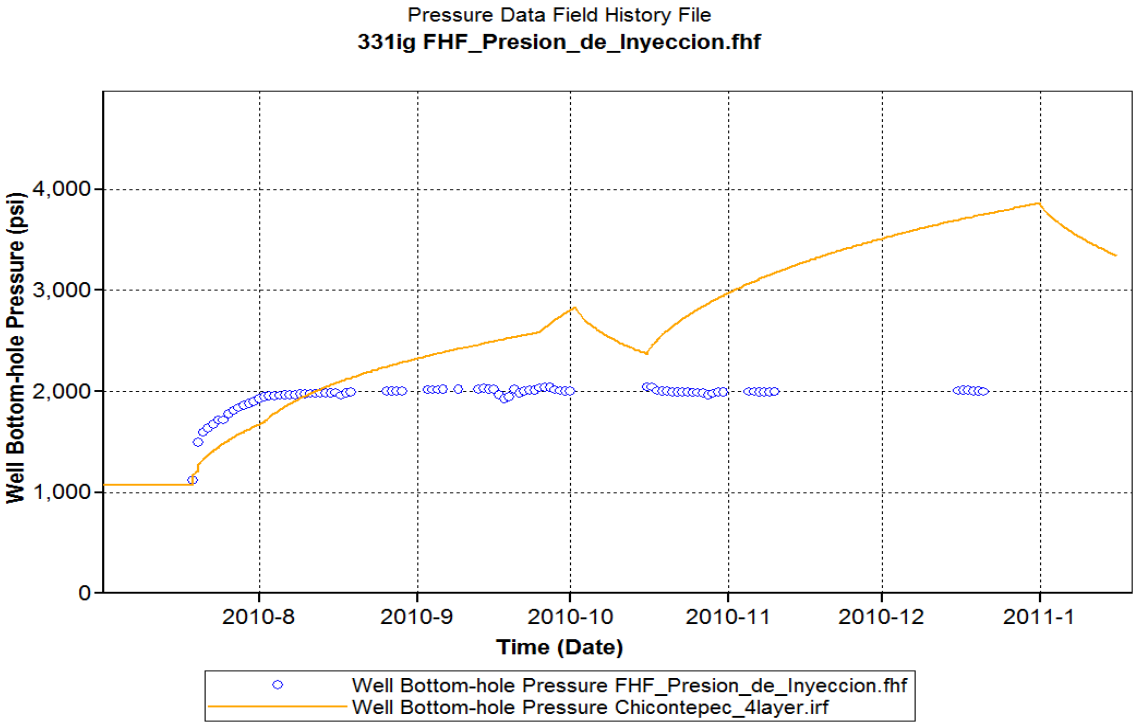

Figure 32: Base case: calculated injection bottom hole pressure. Blue dots represent measured data, the yellow line the calculated BHP.

The next step in history match required to understand how the early CO_2 breakthrough occurred. Based on Hall plot analysis, the fracture pressure and the injection BHP behavior, we decided to simulate several scenarios for extended fractures and geometries. In order to support the idea, we have to look at the evidence.

The Hall plot for the injector well (Fig. 33) shows a change in injectivity, and based on its theory, it is likely that it is due to a fracture extension. In the hall plot, any deviation from the initial trend denotes a change in injectivity due to different factors. If the change is an almost horizontal trend, then it suggests fracturing near the well. If the change deviates in an upward, almost vertical trend, then it suggests well bore plugging. On the other hand, if it creates a slight downward deviation, but away from the horizontal, it

suggests fracture extension (Fig 34). In our study case, this change happens within 50 to 60 days of the start of the injection, and it suggests fracture extension.

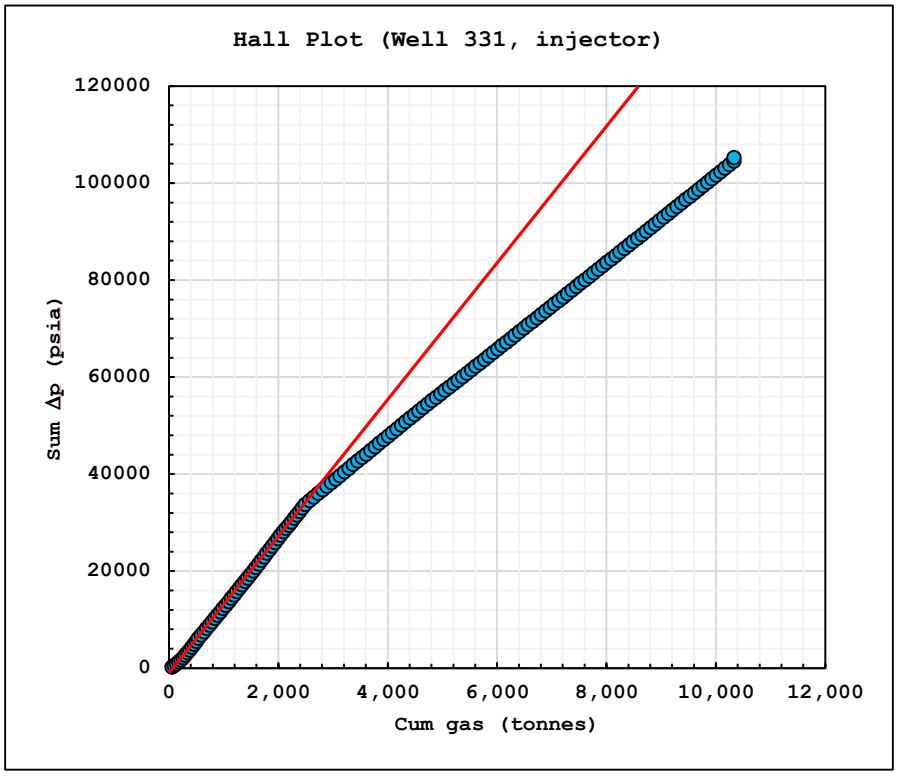

Figure 33: Hall plot for Well 331, CO_2 injector.

It is important to note that the Hall plot theory was developed for a particular incompressible fluid, water. Therefore, one must note that it could not readily apply for any CO_2 plot, other than as diagnostic tool. Now, in our case, CO_2 is pumped downhole in critical and super critical state. For these injection pressures and temperature, CO_2 behaves slightly as an incompressible fluid, and therefore, this methodology may be applied.

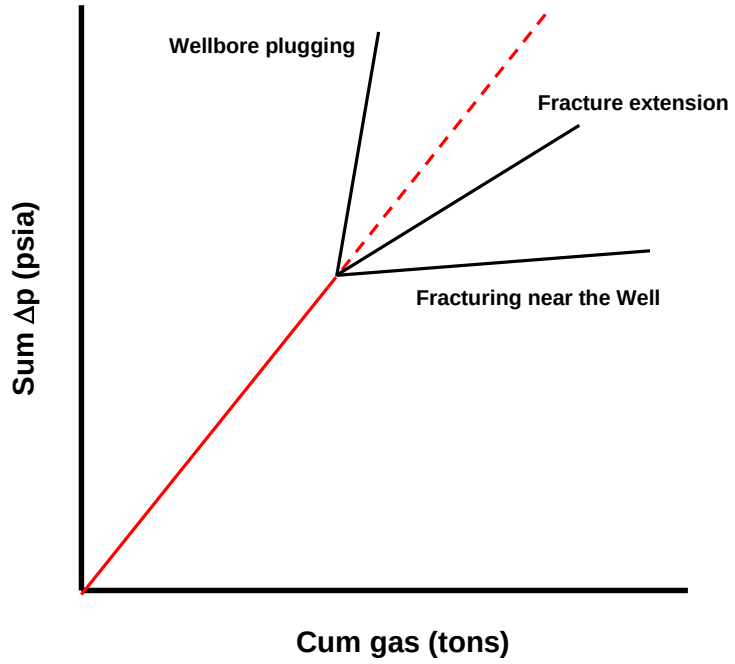

Figure 34: Hall plot theory, adapted from Jarrel and Stein (1991)

On the other hand, the injection BHP profile (Fig. 35) shows a pressure decrease that later recovers in the same timeframe as that of the injectivity change observed in the Hall plot.

An additional aspect to consider, is the role of the rock's fracture pressure, which has been measured at 1730 psi. Combining all of what we have found, we believe that the hydraulic fractured has reached an initial length that stays open thanks to the proppant. When CO_2 starts entering the fracture, there is a small amount of CO_2 that permeates into the formation, losing pressure within the fracture while the bottom hole gauge measures 2000 psi. At some point, the inflow and outflow relative balances, allowing for the CO_2 to reach the tip of the fracture at a sufficiently high pressure, then creating an enlarged fracture.

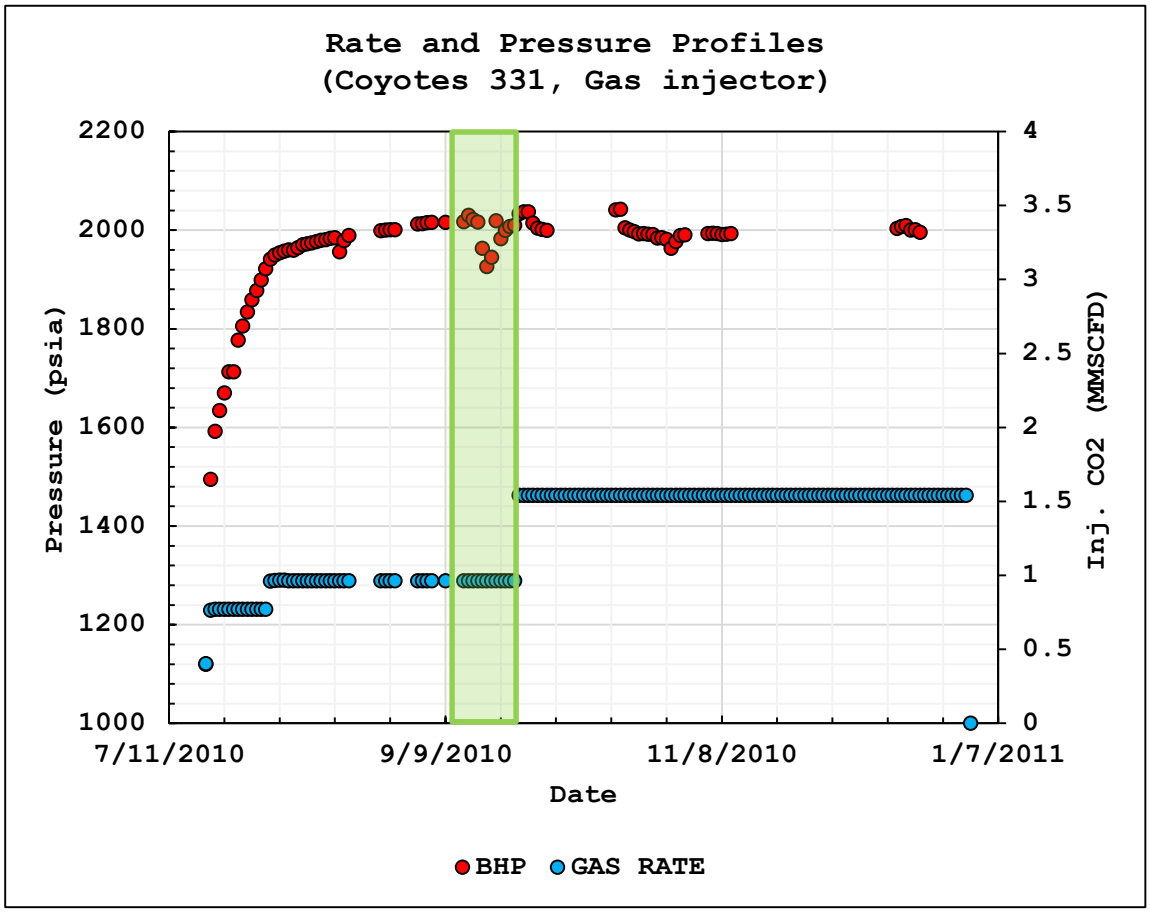

Figure 35: Well 331 injection BHP, CO_2 injector. Shaded in green the time frame at which the Hall plot suggests a change of injectivity.

Now, an enlarged fracture scenario would actually explain how early CO_2 breakthrough occurred, allowing for closer fracture planes or even tip-to-tip communication.

Having explained how early CO_2 breakthrough might have occurred, we decided to implement our ideas in the simulation model. Several scenarios for different fracture lengths and geometries were run and compared to our injection data. We obtained two great matches from a pressure-control and rate-control perspectives (Figs. 36 and 37).

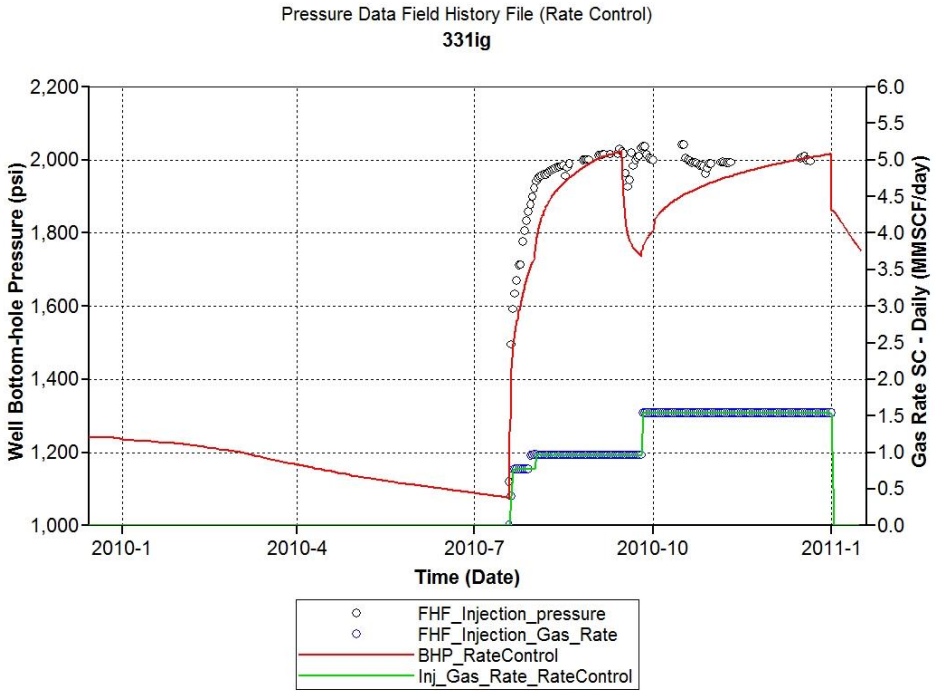

Figure 36: History match, injection rate control.

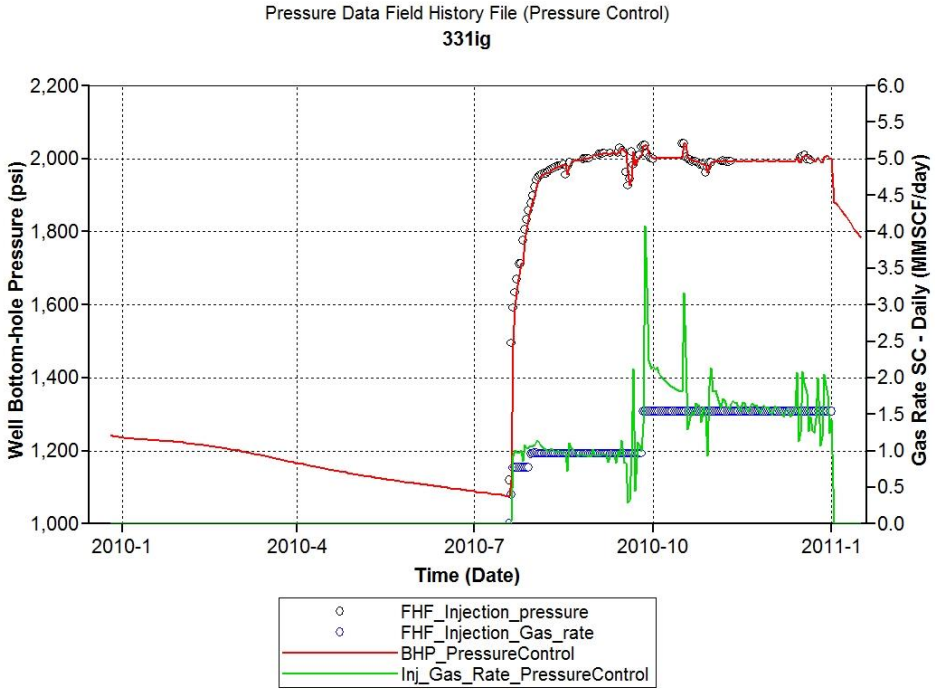

Figure 37: History match, injection BHP control.

We consider the pressure control scenario as our best match. The difference of the historical cumulative CO2 injected and the calculated is of about 10% (Fig. 38), which is within the realm of uncertainty of this study.

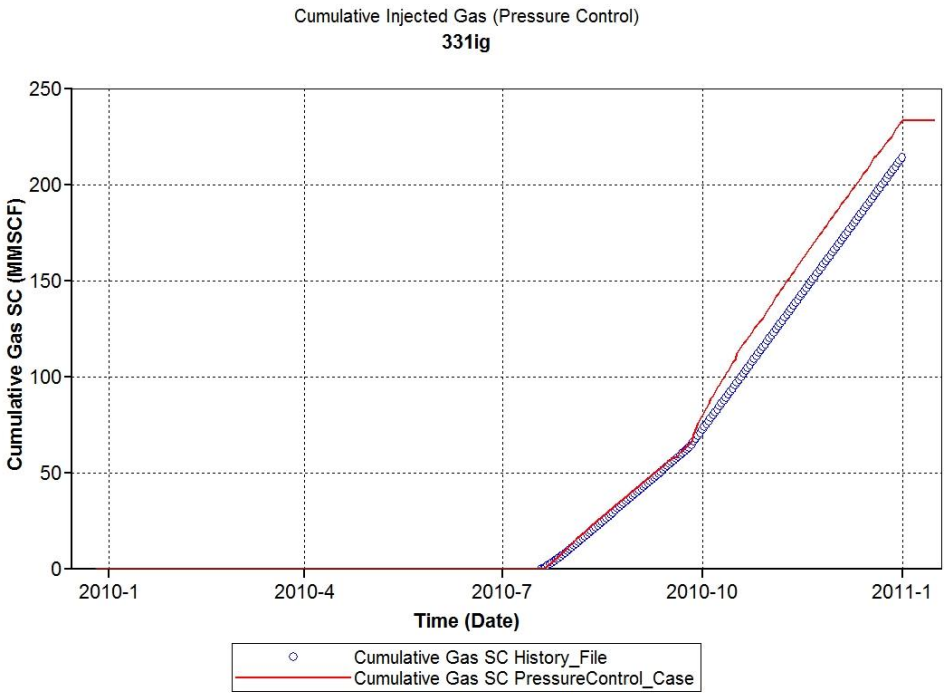

Figure 38: Cumulative CO_2 injected. HM scenario, pressure control.

The match was obtained from one scenario: aligned fractures between the injector and the producer well with tip-to-tip communication. This would explain early BT and simulation runs actually show CO_2 production within the estimated BT timeframe (we must remember that the oil sampling occurred after CO_2 BT).

Forecast and Post Simulation Analysis

Calculated HCPV is of 15.2 MMbbl. Total CO_2 injected is equal to 181.8 Mbbl. This represents less than 1% of HCPV, or in other words, the CO_2 occupied less than 1% of the HCPV. 7 months of production precede CO_2 injection, accounting for most of the cumulative production at the end of the 12 month period, which stands at 97.5 Mbbl.

At first, the test was declared unsuccessful, as early CO_2 BT apparently "gassed" a production well, and production increase was not observed in any of the wells during the 5 month injection period. Nevertheless, history match efforts have shown that tip-to-tip communication between fractures existed, creating an unexpected problem for the project supervisors.

Now, we will answer the following question: What would have happened if we did not stop injection? In order to do that, several cases were run.

- Continued injection of 1.5 MMSCFD of CO_2 for 5, 10, 15 and 20 years.
- Continued injection of 3.0 MMSCFD of CO_2 for 5, 10, 15 and 20 years.
- Continued injection of 4.5 MMSCFD of CO_2 for 5, 10, 15 and 20 years.

By doing so, we were able to create a dimensionless plot which allows us to analyze the dimensionless recovery as a function of dimensionless injection.

Table 11: Oil recoveries from EOR, after 20 years of CO_2 Injection.

Daily CO_2 Injection (MMCFD)	***Cum. Oil from EOR (bbl)****	***Cum. Gas Injected (bbl)****	***EOR Recovery Factor (fraction)***
1.5	2.55×10^6	8.92×10^6	0.19
3.0	3.33×10^6	1.42×10^7	0.26
3.5	3.96×10^6	1.95×10^7	0.31

Fig. 39 is a dimensionless analysis plot for CO_2 flooding, generated from a hypothetical scenario of a higher injection rate and it agrees with our previous conclusion: too little CO_2 was made available into the reservoir.

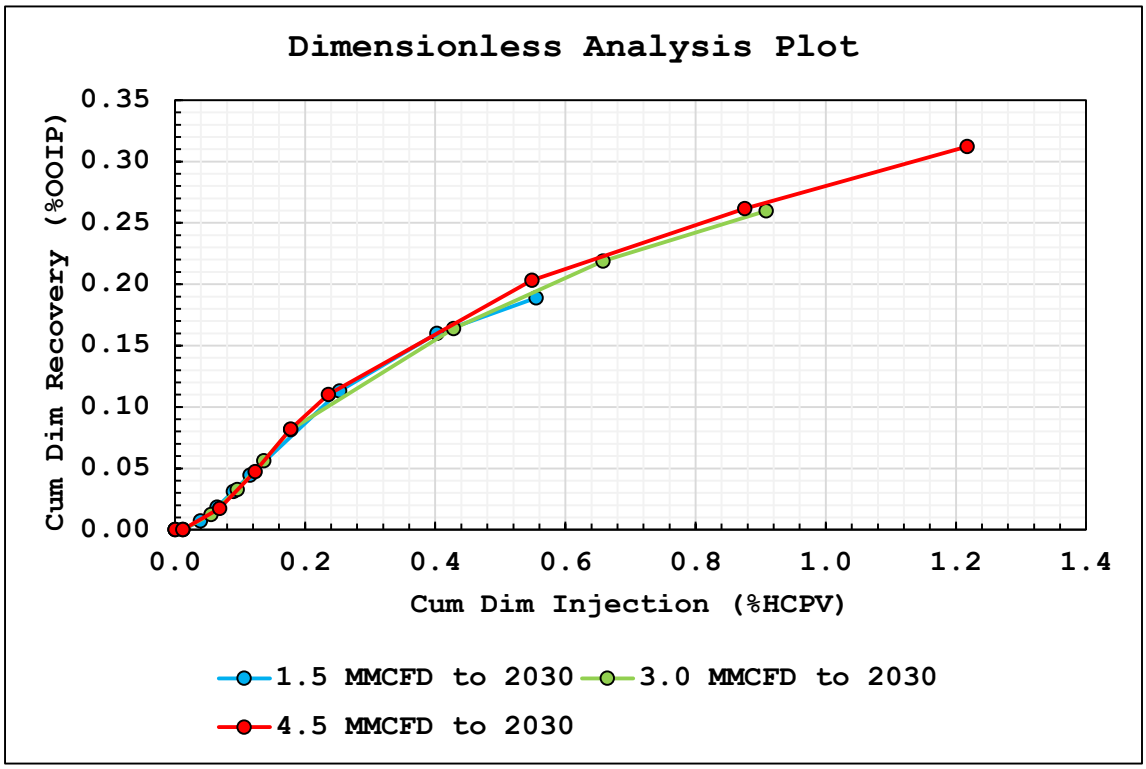

Figure 39: Dimensionless recovery curve.

Fig. 40 shows the expected production response from three injection scenarios: 1.5, 3.0 and 4.5 MMSCFD during the 20 years following the pilot test. We know for certain that 1.5 MMSCFD can be injected with no significant injectivity change, therefore we can take it as our best forecast. On the other hand, assuming that 4.5 MMSCFD could be made available at the reservoir, big production gains could be achieved.

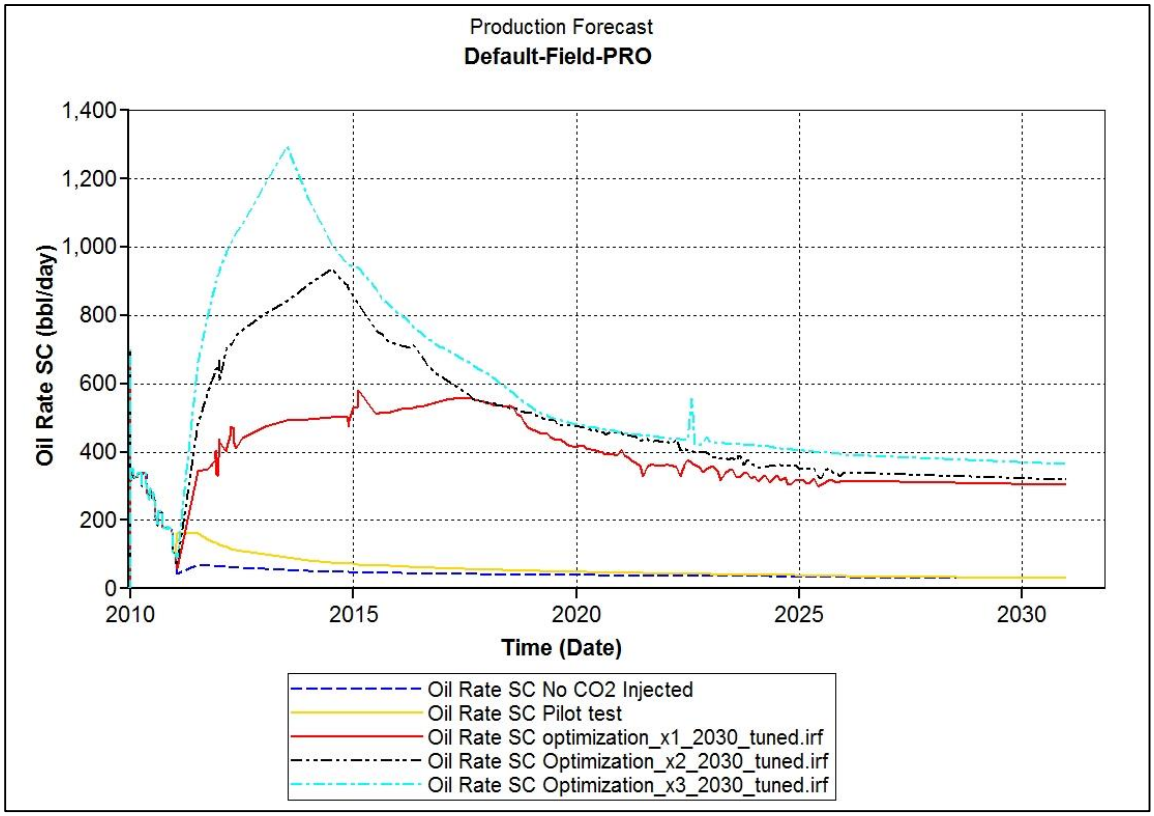

Figure 40: Production profiles for three injection rates.

CHAPTER IV

CONCLUSIONS AND RECOMMENDATIONS

This section discusses our findings, and future work recommendations. Also, a general guideline for performing future projects will be provided.

Conclusions

CO_2 has proven its effectivity in the lab and on the field for various years now. Once it comes into contact with oil, it allows it to flow more easily. Also, its availability and cost makes it an attractive alternative to other processes.

During the execution of the Chicontepec CO_2 pilot test, several questions arose, but the biggest unknown was whether the reservoir is hydraulically continuous or not within 400 m (1312 ft), the well spacing. The lenticular model assumes that it is not, with small lenses (~100 m) of oil impregnated rock randomly located in the Chicontepec basin. However, turbidites are associated with channel-like deposition environments (Mutti and Ricci Lucci 1992), and that allows for longer, elongated sand bodies with varying lengths and thicknesses.

We have shown that there is indeed hydraulic continuity between neighboring wells and that opens for new alternatives, such as that of continuous CO_2 flooding, to increase the performance of this reservoir. The next logical step to further understand the reservoir geology is to get an idea of how far does the hydraulic communication go, instead

of questioning its existence, and aim for long term projects that benefit from CO_2's noble properties.

Now, from this study, we can conclude the following:

1. The pilot test was, in the worst case, inconclusive in testing the CO_2 effectivity as a displacing agent for the Chicontepec field. Valuable insight on the CO_2 interaction with the reservoir was obtained and this should drive future projects.
2. CO_2 HCPVI was too small. CO_2 should be injected at larger volumes to observe any significant production response at the offset wells.
3. Early CO_2 BT does not mean that the test was a failure. As it has been proven, the injection pressure was higher than the fracture pressure, creating an extended fracture that eventually managed to create a conduit from the injector well to one offset well.
4. While it has not been mentioned, as it was not the motive of this study, commercial volumes can be obtained from Chicontepec wells. The case of the Well 333 shows that it is indeed possible at attractive oil rates. Better rock quality and/or better hydraulic fracturing jobs could be the underlying reason. A more detailed study is recommended along with a better coring program.
5. During CO_2 injection simulation, CO_2 movement from the fracture to the reservoir was somewhat slow. Small injection volumes and preferential movement through the fracture seem to be cause behind that, along low permeabilities and their high contrast.

6. If the test would have been executed in lower sand bodies, perhaps, the injection pressure would not surpass the fracture pressure. Further studies should be perform to evaluate this possibility.
7. Good potential is observed in simulation forecasts. Future projects should aim to inject CO_2 for longer periods, while accurately tracking its movement.
8. It is likely that CO_2 injection data was not monitored properly. HM suggests that sometime during the test, CO_2 injection rates were higher than reported. The 10% error observed in Fig. 38 is within the realm of uncertainty of this study.

Recommendations

Several authors have shown the importance of data monitoring during CO_2 flooding. One of the most important parameters, the GOR, was not properly measured and tracking the CO_2 during the test was barely attempted. It is of the utmost importance to have good measurements of the oil and gas rates and to really involve the field staff to get good quality data.

As a rule of thumb, the more quality data we have, the better understanding of the reservoir performance. Enhanced oil recovery processes depend on that rule.

As part of this study, we created a guideline for the required information during any CO_2 flooding. Table 12 shows the recommended information acquisition program as well as the information that should be made available prior to the execution pilot test.

Table 12: Suggested data acquisition program

Data	*Source*	*Frequency*
GOR	From liquid and gas rates	Daily
Well liquid rates	Individual separator or flowmeter measurements	Daily
Well gas rates	Individual separator or flowmeter measurements	Daily
CO_2 injection rates	Surface pumping rates	Daily
Injector BHP	Downhole gauge	Hourly
Producers BHP	Downhole gauge	Hourly
Pre-flooding compositional analysis	At least, recombined surface sample	One, before flooding
During-flooding compositional analysis	At least, recombined surface sample	Once a week, based on the GOR behavior.
Permeability data	Well core data	Before the flooding, for the simulation model

A final recommendation would be as follows: during CO_2 flooding, budgetary constraints or tight deadlines may affect the priorities of the management and they may be tempted to cancel the project within a short time frame. Once in execution, a CO_2 project should be continued unless unfavorable, hard evidence dictates the contrary. If we keep track of the HCPVI, and we observe that it still represents a small percentage of the HCPV, it is recommended to keep injecting. CO_2 has been proven to be effective, with several successful projects still going around the world, and it will not behave differently if we have done our due diligence during the screening process and simulation forecasts. Sound reservoir engineering will always drive the success of our projects.

REFERENCES

Barrufet, M. A. 2015. PETE 644 Lectures. Texas A&M University, College Station, Texas. (Spring 2015)

Caudle, B. H., and Witte, M. D. 1959. Production Potential Changes During Sweep-Out in a Five-Spot System. *Journal of Petroleum Technology*, **12** (12): 63-65. SPE-1334-G. http://dx.doi.org/10.2118/1334-G

Cheatwood, C. J. and Guzman, A. E. 2002. Comparison of Reservoir Properties and Development History: Spraberry Trend Field, West Texas and Chicontepec Field, Mexico. Presented at the SPE International Petroleum Conference and Exhibition, Villahermosa, Mexico, 10-12 February. SPE-74407-MS. http://dx.doi.org/10.2118/74407-MS

Cinco-Ley, H. and Samaniego-Verduzco, F. 1981. Transient Pressure Analysis for Fractured Wells. *Journal of Petroleum Technology*, **33** (9): 1749-1766. SPE-7490-PA. http://dx.doi.org/10.2118/7490-PA

CMG User's Guide – GEM: Advanced Compositional and Unconventional Reservoir Simulator. 2013. Computer Modeling Group Ltd. (CMG). Calgary, Canada.

Comisión Nacional de Hidrocarburos. 2010. Factores de Recuperación de Aceite y Gas en México. DT-1, Comisión Nacional de Hidrocarburos, Ciudad de México, México.

Dindoruk, B. *et al.*, 2005. Improved MMP Correlations for CO_2 Floods Using Analytical Gasflooding Theory. *Journal of Petroleum Technology*, **8** (5): 418-425. SPE-89359-PA. http://dx.doi.org/10.2118/89359-PA

Eclipse. 2014. Eclipse Reservoir Simulation Software Technical Description, version 2014.1. Schlumberger.

Ertekin, T. *et al.*, 2001. *Basic Applied Reservoir Simulation*, first edition. Richardson, Texas. Society of Petroleum Engineers.

Gachuz-Muro, H. *et al.*, 2004. Integrated Characterization of Low Permeability, Submarine Fan Reservoirs for Waterflood Implementation, Chicontepec Fan System, Mexico. Presented at the SPE International Petroleum Conference in Mexico, Puebla, Mexico, 7-9 November. SPE-92077-MS. http://dx.doi.org/10.2118/92077-MS

Holm, L. W. 1976. Status of CO_2 and Hydrocarbon Miscible Oil Recovery Methods. *Journal of Petroleum Technology*, **28** (1): 76-84. SPE-5560-PA. http://dx.doi.org/10.2118/5560-PA

Holm, L. W. 1982. CO_2 Flooding: It's Time Has Come. *Journal of Petroleum Technology*, **34** (12): 2739-2745. SPE-11592-PA. http://dx.doi.org/10.2118/11592-PA

Holm, L. W. and Josendal, V. A. 1974. Mechanisms of Oil Displacement by Carbon Dioxide. *Journal of Petroleum Technology*, **26** (12): 1427-1438. SPE-4736-PA. http://dx.doi.org/10.2118/4736-PA

Jarrel, P. M. and Stein, M. H. 1991. Maximizing Injection Rates in Wells Recently Converted to Injection Using Hearn and Hall Plots. Presented at the SPE Production Operations Symposium, Oklahoma City, Oklahoma, 7-9 April. SPE-21724-MS. http://dx.doi.org/10.2118/21724-MS

McCain Jr, W.D. 2015. PETE 605 Lectures. Texas A&M University, College Station, Texas. (Spring 2015)

Mungan, N. 1981. Carbon Dioxide Flooding – Fundamentals. *Journal of Canadian Petroleum Technology*, **20** (1): 87-92. PETSOC-81-07-03. http://dx.doi.org/10.2118/82-06-07

Mungan, N. 1981. Carbon Dioxide Flooding – Applications. *Journal of Petroleum Technology*, **21** (6): 112-117. PETSOC-82-06-07. http://dx.doi.org/10.2118/81-01-03

Mutti, E.: "Turbidités Et Cones Sous-Marine Profonds". In Homewood, P. (ed.), Sedimentation Detritrique (fluviatile, littorale et marine). Institute de Geologie, Universite de Fribourg, Fribourg Switzerland, pp. 353-419. 1979.

Mutti, E.: "Turbidite Sandstones". AGIP-Istituto di Geologia, Universitá di Parma, Italy, pp. 275.1992

Mutti, E. and Ricci Lucci, F.: "Le Torbiditi Dell' Apennine Settentrionale: Introduzione All' Analisi Di Facies". Memorie Societa Geologica Italiana, Vol. 11, pp. 161-199 (translated into English by T. H. Nilsen, 1978. International Geology Review, Vol. 20, No. 2, pp. 125-166. 1972.

PEMEX. 2015. Reservas de Hidrocarburos de México al 1 de Enero de 2015. Public Report, PEMEX, Ciudad de México, México.

PEMEX, 2015. United States Securities and Exchange Commission 20-F Report. Public Report. PEMEX, Ciudad de México, México.

Ramey Jr., H. J. e*t al*., 1981. Effect of Non-Darcy Flow on the Constant-Pressure Production of Fractured Wells. *Society of Petroleum Engineers Journal*, **22** (3): 390-400. SPE-9344-PA. http://dx.doi.org/10.2118/9344-PA

Ramey Jr., H. J. e*t al*., 1982. Non-Darcy Flow in Wells with Finite-Conductivity Vertical Fractures. *Society of Petroleum Engineers Journal*, **22** (5): 681-698. SPE-8281-PA. http://dx.doi.org/10.2118/8281-PA

Rangel-German, E. 2012. IOR-EOR: El Futuro de la Producción de Aceite en México: Recuperación Avanzada y Mejorada. Public Report, Comisión Nacional de Hidrocarburos, Ciudad de México, México.

Salazar, U., Cinco, H. and Castro, I. 2011: *Productividad de Pozos en Yacimientos Areno-Arcillosos: Caso Chicontepec*. B.S. Dissertation, Universidad Nacional Autónoma de México, Ciudad de México, México. (June 2011)

Sebastian, H. M. *et al.*, 1985. Correlation of Minimum Miscibility Pressure for Impure CO_2 Streams. *Journal of Petroleum Technology*, **37** (11): 2076-2082. SPE-12648-PA. http://dx.doi.org/10.2118/12648-PA

Silva, M. K. and Orr Jr, F. M. 1987. Effect of Oil Composition on Minimum Miscibility Pressure – part 1: Solubility of Hydrocarbons in Dense CO_2. *SPE Reservoir Engineering*, **2** (4): 468-478. SPE-14149-PA. http://dx.doi.org/10.2118/14149-PA

Silva, M. K. and Orr Jr, F. M. 1987. Effect of Oil Composition on Minimum Miscibility Pressure – part 2: Correlation. *SPE Reservoir Engineering*, **2** (4): 479-491. SPE-14150-PA. http://dx.doi.org/10.2118/14150-PA

Society of Petroleum Engineers. SPE *Style guide 2015-2016*. 2015, SPE.

Stosur, G. J. *et al*., 2003. The Alphabet Soup of IOR, EOR and AOR: Effective Communication Requires a Definition of Terms. Presented at the SPE International Improved Oil Recovery Conference in Asia Pacific, Kuala Lumpur, Malaysia, 20-21 October. SPE-84908-MS. http://dx.doi.org/10.2118/84908-MS

The Free Dictionary, By Farlex. Carbon Dioxide, (2011 revision), http://www.thefreedictionary.com/carbon+dioxide (accessed 24 May 2016)

Thomas, S. 2008. Enhanced Oil Recovery – An Overview. *Oil and Gas Science and Technology*, **63** (1): 9-19. IFP. http://dx.doi.org/10.2516/ogst:2007060

Yellig, W. F. and Metcalfe, R. S. 1980. Status of CO_2 and Hydrocarbon Miscible Oil Recovery Methods. *Journal of Petroleum Technology*, **32** (1): 160-168. SPE-7477-PA. http://dx.doi.org/10.2118/7477-PA